Linnaeus University Dissertations
No 329/2018

Natacha Ndizeye

New Strategies for Preparing Polymers with Hierarchical Architectures

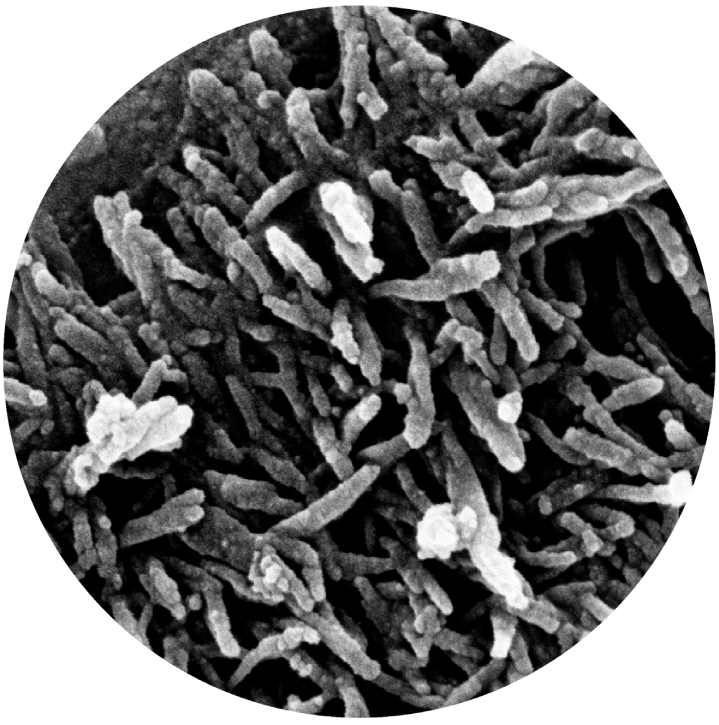

LINNAEUS UNIVERSITY PRESS

New Strategies for Preparing Polymers with Hierarchical Architectures

Linnaeus University Dissertations
No 329/2018

New Strategies for Preparing Polymers with Hierarchical Architectures

Natacha Ndizeye

LINNAEUS UNIVERSITY PRESS

New Strategies for Preparing Polymers with Hierarchical Architectures
Doctoral Dissertation, Department of chemistry and biomedical sciences,
Linnaeus University, Kalmar, 2018

ISBN: 978-91-88761-96-5 (print), 978-91-88761-97-2 (pdf)
Published by: Linnaeus University Press, 351 95 Växjö
Printed by: DanagårdLiTHO, 2018

Abstract

Ndizeye, Natacha (2018). *New Strategies for Preparing Polymers with Hierarchical Architectures,* Linnaeus University Dissertations No 329/2018, ISBN: 978-91-88761-96-5 (print), 978-91-88761-97-2 (pdf). Written in English.

The objective of this thesis was to explore novel approaches for controlling morphologies and molecular recognition behaviour of polymers and to use these strategies in conjunction with the molecular imprinting technique in order to either enhance polymer performance in quartz crystal microbalance (QCM) sensor applications, or as an alternative to conventional solvents of polymerization. In **Papers I** and **II**, the use of liquid crystalline media in the synthesis of molecular imprinted polymers was demonstrated. When used in conjunction with the molecular imprinting technique the LC media induced hierarchical material architectures, which provided an enhancement of QCM-sensor sensitivity. The use of a class of novel solvents, so-called "non-ionic deep eutectic solvents (ni-DESs)", was explored in polymer synthesis, **Paper III**, and for molecularly imprinted polymer synthesis, **Paper IV**. The use of these solvents produced polymers with morphological features comparable to those prepared in conventional solvents, and sensitivities towards bupivacaine template were observed. Collectively these results present a new strategy for generating new hierarchical polymer architectures and a new class of solvent for polymer synthesis, which can also be used for molecular imprinting, that can be used as an alternative to conventional and sometimes flammable or toxic polymerization solvents.

Keywords: Liquid crystalline media, molecularly imprinted polymers, non-ionic deep eutectic solvents, quartz crystal microbalance

To my belated dad whom I miss dearly

Svensk populärvetenskaplig sammanfattning

I denna avhandling utforskas nya metoder för att reglera både strukturen hos polymerer och deras molekylära igenkänning. Tillämpning av dessa metoder i samband med molekylavtryckstekniken gör det möjligt att förbättra polymerernas egenskaper i sensortillämpningar och att ersätta vanliga lösningsmedel för polymerframställning.

I **arbete I** och **II** användes flytande kristaller som lösningsmedel vid framställning av polymerer. När de flytande kristallerna användes i samband med molekylavtryckstekniken bildades ordnande strukturer i polymererna, vilket gav en ökning av känsligheten i en sensor.

En klass av nya lösningsmedel, så kallade "icke-joniska djupa eutektiska lösningsmedel", användes för polymerframställning i **arbete III** och i samband med molekylavtryckstekniken i **arbete IV**. Strukturen hos de polymerer som framställdes med hjälp av dessa lösningsmedel var jämförbar med den hos polymerer som framställts i traditionella lösningsmedel, och molekylavtryckstekniken fungerade som förväntat.

Tillsammans demonstrerar dessa resultat en ny metod för att påverka strukturen hos polymerer och en ny klass av lösningsmedel som alternativ till konventionella, ibland brandfarliga eller toxiska lösningsmedel för polymerframställning.

List of publications

This thesis is based on following publications, which are referred to by their roman numerals in the text. All papers are reproduced with permission from the respective publisher.

I. Suriyanarayanan, S., Nawaz, H., Ndizeye, N. & Nicholls, I.A. (2014). Hierarchical thin film architectures for enhanced sensor performance: liquid crystal-mediated electrochemical synthesis of nanostructured imprinted polymer films for the selective recognition of bupivacaine. *Biosensors*. 4: 90-110.

II. Ndizeye, N., Suriyanarayanan, S. & Nicholls, I.A. (2018). Hierarchical polymeric architectures through molecular imprinting in liquid crystalline environments. *European Polymer Journal*. 106: 223–231.

III. Ndizeye, N., Suriyanarayanan, S. & Nicholls, I.A. Polymer synthesis in non-ionic deep eutectic solvents. *Submitted.*

IV. Ndizeye, N., Suriyanarayanan, S. & Nicholls, I.A. Molecular imprinting in a non-ionic deep eutectic solvent. *Submitted.*

Additional work outside the scope of this thesis:

Suriyanarayanan, S., Olsson, G.D., Kathiravan, S., Ndizeye, N. & Nicholls, I.A. Non-ionic deep eutectic liquids – acetamide-urea derived room temperature solvents. *Submitted.*

Abbreviations

AA	Acetamide
ABAH dihydrochloride	2,2′-Azobis(2-methylpropionamidine)
AIBN	2,2′-Azobis(2-methylpropionitrile)
AOT	Dioctyl sodium sulfosuccinate
APBA	3-Aminophenylboronic acid
BAP	1,4 Bis(acryloyl)piperazine
BET	Brunauer-Emmett-Teller
DVB	Divinylbenzene
EGDMA	Ethylene glycol dimethacrylate
FT-IR	Fourier transform infrared spectroscopy
HEMA	Hydroxyethylmethacrylate
LC	Liquid crystalline
MAA	Methacrylic acid
MIP	Molecularly imprinted polymer
Ni-DES	Non-ionic deep eutectic solvent
NMA	*N*-methylacetamide
NMU	*N*-methylurea
NN'DMU	*N*,*N'*-dimethylurea
p-PD	*p*-Phenylenediamine
QCM	Quartz crystal microbalance
REF	Reference polymer
SEM	Scanning electron microscopy
Tx-100	Triton X-100

Table of Contents

1. INTRODUCTION

New materials are essential for resolving societal challenges ranging from the need for better health care and security to energy management, through their use in more sensitive and robust detection systems and for limiting energy consumption and for energy storage [1]. For use in such applications, the physico-chemical properties of materials need to be engineered to allow for the integration of the material into its operating environment and to optimize its function. To achieve these requirements, methods are needed for controlling material properties over the Ångström- to micrometer-scale, which in turn necessitates understanding and directing molecular recognition events. In this thesis new molecular recognition-based strategies are explored aimed at producing polymeric materials with pre-determined physico-chemical properties over this size range.

1.1 Molecular recognition

Molecular recognition is described as the interaction between one molecule, the host, and another target molecule, the guest, with high specificity and affinity to form a specific complex through non-covalent interactions, such as electrostatic interactions, hydrogen-bonds, hydrophobic interactions and van der Waals forces [2]. These host-guest relationships play a key role in biological systems and they are essential for the existence of life. Biological systems rely on the ability of biomolecules to specifically recognize each other. Many examples of molecular recognition exist in nature such as the antigen-antibody recognition in the immune system, the binding of an enzyme to a substrate, protein-deoxyribonucleic acid (DNA) and ribosome-ribonucleic acid (RNA) interactions.

1.1.1 Biomolecular recognition

Antibodies, also known as immunoglobulins (Igs), are the most widely studied and best-known examples of biomolecular recognition in nature. Antibodies are large proteins synthesized by the immune system to selectively recognize and neutralize foreign objects, called antigens, that can range from simple proteins to large bacteria and viruses [3]. Each antibody is comprised of two identical light (25 kDa) chains (each containing about 220 amino acids) and two identical heavy (55 kDa) chains (each usually containing about 440 amino acids). The four chains are held together by disulfide bridges to form a Y shape (Figure 1.1, left). The variable regions of an antibody form antigen-binding sites (paratope) with specific shapes at the tip of each arm for interaction with the antibody binding sites of an antigen (epitope) and only antigens that match this shape will fit into these binding sites (Figure 1.1, right). This interaction occurs via electrostatic forces, hydrogen bonds, van der Waals forces, hydrophobic forces, or a combination of all these non-covalent interactions. The ability of antibodies to bind to their targets with high affinity and specificity makes them good candidates for therapeutic and diagnostic applications such as detection and quantification of antigen targets and also for treatment of certain diseases [4-6].

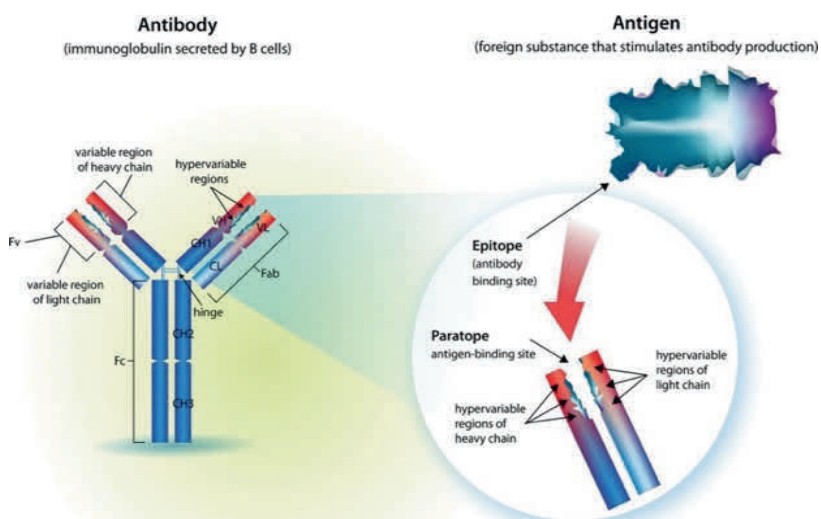

Figure 1.1. Antibody structure (left) and antibody-antigen recognition (right). *Reproduced with permission from [7].*

However, there are some limitations associated with biological recognition elements such as instability and high production cost. For example, antibodies

are fragile, unstable and short-lived outside their native environment, therefore they cannot be used on a large scale or under harsh conditions and these disadvantages limit their use in many applications [8]. Extensive efforts have been focused on the development of synthetic systems mimicking the natural processes of molecular recognition which would be able to overcome the limitations associated with natural systems.

1.1.2 Artificial receptors

In 1967 Pedersen reported the synthesis of cyclic polyethers which he named crown ethers. These molecules are recognized as highly selective compounds which interact with metal ions. They are composed of several repeating units of ethylene oxide which exhibit the binding selectivity for alkali metal and alkali earth metal cations [9]. For example, 18-crown-6 (Figure 1.2, left) has a strong binging affinity for a potassium cation (K^+), 15-crown-5 (Figure 1.2, middle) for sodium cation (Na^+) and 12-crown-4 (Figure 1.2, right) for lithium cation (Li^+).

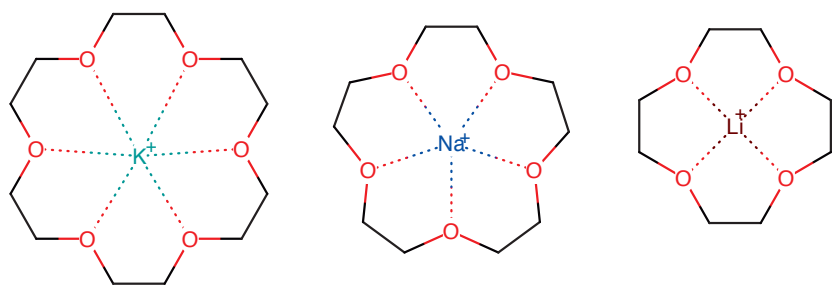

Figure 1.2. Chemical structures of (left) 18-crown-6, (middle) 15-crown-5 and (right) 12-crown-4 crown ethers binding alkali metal ions.

Jean-Marie Lehn in 1969 expanded Pedersen's fundamental discovery by designing cryptands, polycyclic compounds which are three-dimensional analogues of crown ethers resulting in higher selectivity and stronger binding to the guest ions than that achieved with simple crown ethers. An important example of these molecules parallel in size to the 18-crown-6 but exhibiting higher binding selectivity is the [2.2.2] cryptand (Figure 1.3, left). This higher selectivity is believed to be due to the metal ion being held within a three-dimensional "spherical recognition" cavity [10].

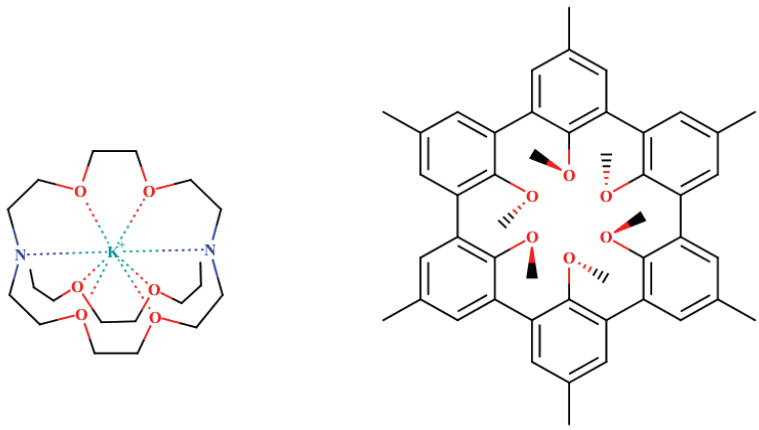

Figure 1.3. Chemical structures of [2.2.2] cryptand complexed with K^+ (left) and spherand (right).

Donald J. Cram provided further development of the area when he introduced spherands, highly stable molecules forming strong complexes of extremely high selectivity. These compounds are composed of multiple aromatic rings of covalently bound phenyl groups with preformed cation binding sites making them inflexible and more rigid in structure than crown ethers and cryptands [11]. The spherand (Figure 1.3, right) is one of the strongest complexants known for Li^+.

Due to their remarkable capacities to form stable complexes with metal ions, non-metal ions, and neutral molecules, crown ethers played a leading role in the development of host-guest chemistry, a term used by Cram and together they are considered the first generation of hosts, representing the birth of supramolecular chemistry, a term coined by Lehn [12]. The work of Pedersen, Cram and Lehn was recognized when they were awarded the Nobel Prize in 1987 “for their development and use of molecules with structure-specific interactions of high selectivity" [13]. Their pioneering work has opened the way for new advances in the area of macrocyclic chemistry, offering new areas for their application including; ion chromatography, phase-transfer catalysis, organic and inorganic synthesis and biochemistry. However, the synthesis of such receptors is complicated, expensive and very time consuming. The development of straightforward techniques for the synthesis of stable alternatives at low cost is desirable. Strategies including the screening of phage display [14] and SELEX libraries [15], which are also subject to the problems associated with biomolecular stability, and combinatorial chemical libraries [16-17] have been developed, though perhaps more promising is the molecular imprinting technique.

1.2 Molecular imprinting

Molecular imprinting is a technique for creating highly selective polymeric receptors in synthetic polymers. These molecularly imprinted polymers (MIPs) possess ligand-recognition characteristics reminiscent of those of biological counterparts, *e.g.* antibody-antigen recognition [18]. This has led to MIPs often being referred to as artificial antibodies, synthetic receptors, and even as enzyme mimics in cases when they demonstrate catalytic properties. Common to MIPs is that they selectively recognize and bind a target molecule, often with affinities and specificities comparable to those observed in biology.

In this method, a well-defined composition of polymerizable functional monomers and cross-linking monomers are co-polymerized in the presence of the template molecule, in a porogenic solvent chosen to solubilize and stabilize the pre-polymerization mixture. After polymerization, the template is removed from the polymeric structure by washing with a suitable solvent, revealing recognition sites that are complementary to the template in terms of size, shape and functionality; this enables subsequent recognition of the template, or a structural analogue, during the rebinding process [19]. The concept behind the formation of the selective binding sites is schematically shown in Figure 1.4.

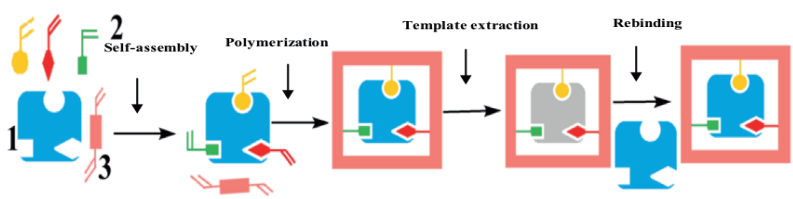

Figure 1.4. Schematic illustration of the molecular imprinting principle. 1: template (blue), 2: monomers (yellow, red and green) and 3: cross-linker (pink) self-assemble in the pre-polymerization mixture. After polymerization, the template is extracted resulting in a polymer with recognition sites able to rebind again the template molecule.

There are many parameters that influence the molecular imprinting process and impact on MIP performance. Thus, the nature of the template, and the choice of the chemical reagents *i.e.* functional monomer, cross-linker and solvent is crucial in order to get efficient functional MIPs, as are temperature and pressure [20-21]. The template is at the center of MIP preparation and the choice of functional monomer is critical as it must have chemical groups that

can interact with complementary functional groups of the template. The most commonly used functional monomers in MIP synthesis participate in hydrogen bonding interactions. Cross-linkers are responsible firstly for fixing and controlling the morphology of the polymer complex, secondly for stabilizing the imprinted binding sites and lastly for providing mechanical stability and cavity rigidity in the resultant polymer. The functional monomer to cross-linker ratio should be high enough to maintain stability and the porousness of the recognition sites thus the greater degree of cross-linker the more rigid the polymer. The most frequently used method for the preparation of imprinted polymers is the free radical polymerization that is triggered by an initiator either by thermolysis (heat), photolysis (UV radiation) or by chemical/electrochemical means. The porogen is responsible for bringing together all pre-polymerization components (template, monomer, cross-linker, initiator) and to form pores in the macroporous polymers. In addition, the porogen should also stabilize the template-monomer complex formation in non-covalent imprinting [22-24].

There are three different approaches for synthesizing MIPs, which differ in the nature of the interactions between the template molecule and functional monomers involved in the imprinting and rebinding steps: the covalent, non-covalent and semi-covalent approaches. The covalent approach involves the formation of covalent bonds between the template and the functional monomers prior to polymerization; the template is then chemically cleaved from the resultant polymer. During the rebinding process, the covalent bonds are re-formed to bind the template to the polymer network. Wulff *et al.* reported the first example of covalent imprinting [25], using 4-nitrophenyl-α-D-mannopyranoside conjugated to *p*-vinylbenzeneboronic acid as template, and co-polymerized it with methyl methacrylate and ethylene dimethacrylate as a cross-linking monomer. After polymerization, the boronic acid ester was cleaved, and the 4-nitrophenyl-α-D-mannopyranoside was extracted. During the rebinding process it was found that the resultant polymer bound strongly and selectively to the template. This strategy was later further developed by Shea [26]. The main advantage of this method is the homogeneity of the binding sites due to the orientational control and interaction stability provided by covalent bonds. This has been further studied by Shimizu and co-workers [27]. Moreover, this approach accomplishes higher binding constants due to covalent bond types such as boronate ester [28], ketal/acetal [29], and Schiff's base [30]. However, this technique has some drawbacks including the requirement for significant synthetic effort and the oftentimes slow kinetics of bond formation and cleavage making the removal of the template difficult. Moreover, there is a limited number of reversible covalent bond-types available and matching the template and monomers functionalities for covalent imprinting can be difficult. These disadvantages limit the use of this method in many application areas.

In the early 1980's, Mosbach and co-workers introduced a second strategy that became known as non-covalent imprinting [31]. In this approach, the template interacts with a functional monomer through non-covalent interactions, *e.g.* hydrogen bonding, van der Waals forces and ionic or π-π interactions, during the imprinting and rebinding procedures. Prior to polymerization, the template and functional monomers are self-assembled simply by dissolving them in a suitable solvent. The template is removed by washing the prepared MIPs with a suitable solvent or a mixture of solvents and the rebinding process of the template to the imprinted sites is based on non-covalent interactions. Non-covalent imprinting is the predominant method used today due to its simplicity, faster template rebinding, and ease of removal of the template from the polymer. In addition, a large number of functional monomers and crosslinkers are commercially available. The most commonly used functional monomers include methacrylic acid (MAA), trifluoromethylacrylic acid, acrylamide and hydroxyethylmethacrylate (HEMA), and cross-linkers include ethylene glycol dimethacrylate (EGDMA) and divinylbenzene (DVB) Figure 1.5 presents the building blocks for molecularly imprinted polymer synthesis used in this thesis.

The non-covalent technique was used for instance by Haupt *et al.* for imprinting the herbicide 2,4-dichlorophenoxyacetic acid (2,4-D) in the presence of the polar solvents methanol and water using a 4-vinylpyridine-co-EGDMA based polymer system. The complex formation between the template and the functional monomer 4-vinylpyridine relied on the combination of hydrophobic and ionic interactions [32]. However, the non-covalent strategy suffers from some drawbacks including heterogeneity of the recognition binding sites due to the excess use of monomers in order to displace the equilibrium towards the formation of template-monomer complexes, leading to the formation of non-specific binding sites thus diminishing the binding selectivity [33].

In 1995, Whitcombe and co-workers developed a hybrid approach, combining the advantages of the covalent and the non-covalent methods, called semi-covalent imprinting [34]. In this method, the template is covalently coupled to functional monomers during polymerization whereas rebinding takes place with non-covalent interactions. During the semi-covalent imprinting process, a linker group known as "sacrificial spacer" is used between the template and the functional monomer to prevent steric crowding, this linker is removed along with the template. This approach has been used successfully in extraction or clean-up procedures of compounds such as glyceric acid [35], 4-nitrophenol [36] and phenols [37].

Depending on the intended application, MIPs have been prepared in a variety of formats. Traditionally, MIPs have been prepared as monoliths by bulk

polymerization where the resultant monoliths are crushed, ground, sieved to an appropriate particle size and subsequently packed in a chromatographic column. Although this method is simple, the preparation steps are time-consuming, tedious, unsuitable for large-scale production, and the ground particles are irregular in size and shape. To overcome the perceived drawbacks of bulk polymerization, more sophisticated MIP formats such as (nano)monoliths, fibres, nanoparticles, beads, membranes and thin films have been developed using various synthetic strategies including *in situ* polymerization, suspension polymerization, precipitation polymerization, multi-step swelling and surface polymerization [23, 38].

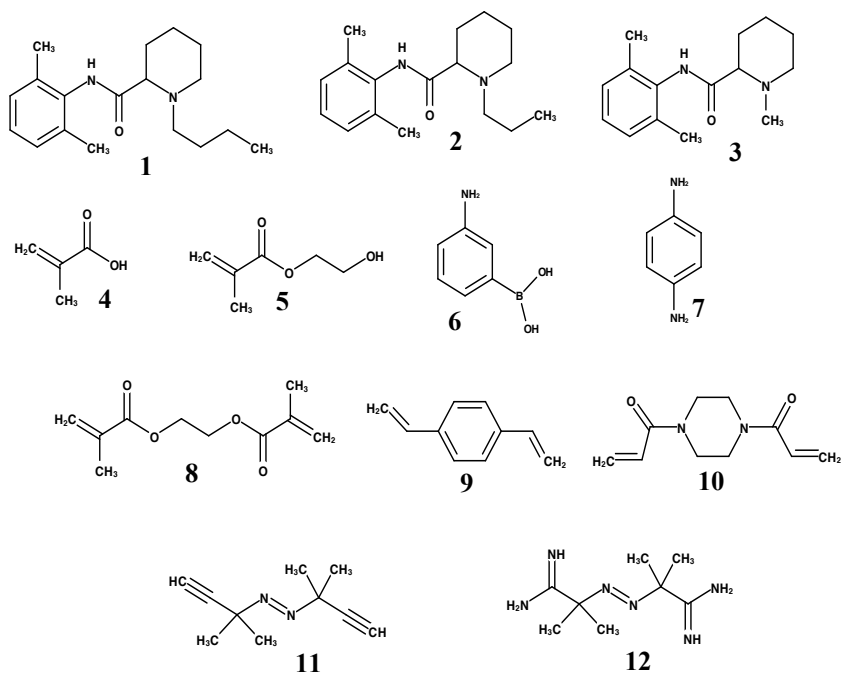

Figure 1.5. Structures of bupivacaine (**1**), ropivacaine (**2**), mepivacaine (**3**), MAA (**4**), HEMA (**5**), 3-aminophenylboronic acid (APBA, **6**), *p*-phenylenediamine (*p*-PD, **7**), EGDMA (**8**), DVB (**9**), 1,4 bis(acryloyl)piperazine (BAP, **10**), 2,2′-azobis(2-methylpropionitrile) (AIBN, **11**) and 2,2′-azobis(2-methylpropionamidine) dihydrochloride (ABAH, **12**).

In comparison to their biological analogues (enzymes, antibodies, and hormone receptors), the advantages of MIPs include their ease of preparation, low cost, high physical and chemical resistance and no requirement for

laboratory animals or hapten conjugation protocols. Moreover, they can be stored for several years at room temperature without losing their performance [23, 39]. These advantages have enabled them to be used successfully in different application areas.

One of the most widely studied areas of MIP applications is their use in analytical separations. MIPs have been utilized as sorbents for solid-phase extraction (SPE) known as molecular imprint-based SPE (MISPE) [40-42]. In 1994, Sellergren was the first to report the use of MISPE where he prepared a pentamidine selective MIP for its online sample enrichment from spiked urine [43]. MIPs have also been used as chiral stationary phases for racemic mixtures in high-performance liquid chromatography (HPLC) in order to get optically pure compounds and fine chemicals [44-46]. For example, baseline separation of D- and L-phenylalanine (Phe) was achieved by employing D-Phe imprinted poly(MAA-co-EGDMA) microbeads as HPLC stationary phase [47].

One interesting application of MIPs is the creation of highly catalytically active polymers or plastic enzymes able to mimic the high affinity binding and specificity of antibodies and enzymes [48-50]. An early example from the Mosbach group involved a MIP able to catalyze the isomerization of benzisoxazole to 2-cyanophenol [51].

MIPs are good candidates for application in therapeutics and medical therapy due do their ability to bind strongly and selectively to bioactive molecules. The use of MIPs in drug delivery systems [52] offers tremendous potential, although with great challenges, *e.g.* biocompatibility. Efforts in this field are being directed, in particular, towards the preparation of MIPs for controlled delivery of drugs. For example, Norell *et al.* prepared theophylline MIPs to examine their potential as a controlled release drug dosage form [53-54], and MIPs have even been used in contact lenses for ocular administration of beta-blockers [55].

MIPs have been employed as antibody and receptor mimics due to their high affinities and specificities, often comparable to those of antibodies and biological receptors [56-60]. The first use of MIPs as an antibody substitute was demonstrated by Mosbach's group in 1993. They prepared a MIP-based assay for theophylline and diazepam using radio-labeled ligands and the results showed strong binding and cross-reactivity profiles similar to those of antibodies [61]. This molecularly imprinted sorbent assay was later used by other groups to develop assay systems for the detection of several compounds *e.g.* morphine [62], (*S*)-propranolol [63], herbicides [64] and corticosteroids [65].

Molecular imprinting techniques have also been utilized for small target ligands and also for macromolecules like proteins [66-67]. For example, protein-imprinted films have been prepared for the detection of low-density lipoprotein [68], bovine hemoglobin and insulin [69] and protein C in human serum [70].

MIPs have been successfully used as artificial recognition elements in biomimetic sensing devices or sensors, in particular piezoelectric quartz crystal microbalance (QCM)-based systems [71-76], though even in electrochemical [77-80], surface plasmon resonance [81-83] and fluorescence-based [84-85] sensor platforms.

1.3 Quartz crystal microbalance

The working principle of a quartz crystal microbalance (QCM) is based upon piezoelectricity (from the Greek "pressure-electric) of quartz crystals. This piezoelectric effect was first published in 1880 by Pierre and Paul-Jacques Curie [86], describing the development of an electrical charge on a crystal in response to an applied mechanical stress (pressure) [87-88]. In a QCM, the application of an alternating voltage to a quartz crystal causes a mechanical oscillation of characteristic frequency resulting in vibrations of the piezoelectric crystal [89-90].

Quartz (Figure 1.6, left), the crystalline form of silicon dioxide (SiO_2), is a naturally occurring piezoelectric material. Quartz crystal is the most commonly used piezoelectric material because of its ready availability, robust mechanical properties, good reliability, long life and in particular its resistance to high temperatures [91]. The manner in which the quartz crystal is cut determines its resonant frequency and its mode of oscillation. The AT-cut is the most popular cut type used for oscillations in the MHz range and it is performed by slicing a quartz rod at an angle of 35°15' to the z-axis of the crystal (Figure 1.6, right) [88]. AT-cut crystals are suitable for sensor devices since their oscillations are very temperature stable within the 10 to 50 °C range [92]. Most quartz crystal transducers have a basic resonant frequency of 5 or 10 MHz although 20 to 30 MHz crystals are sometimes used; however they require more careful handling because their quartz plates are very thin and fragile [93]. Practical difficulties in making very thin quartz crystal plates limit the highest fundamental frequency that can be achieved to 45 MHz. Piezoelectric quartz crystal resonators are also used in common electronic devices such as watches, computers, radars, televisions and cellular phones [94].

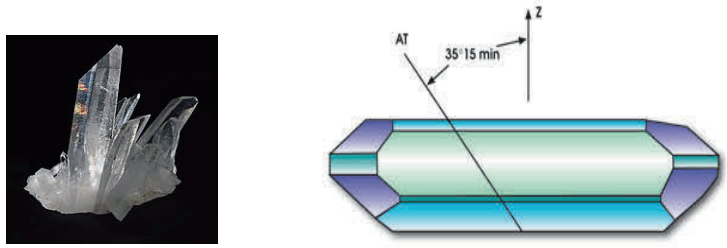

Figure 1.6. Quartz crystal cluster (left) [95] and AT-cut quartz crystal (right) *Copyright © 2018 Laurin Publishing Co., Inc* [96].

When used for QCM, a piezoelectric AT-cut quartz crystal is sandwiched between two electrodes (Figure 1.7, left) and resonates electromechanically in the thickness shear mode (Figure 1.7, right) [97].

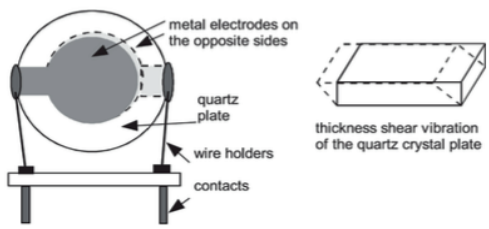

Figure 1.7. A piezoelectric quartz crystal sandwiched between two metal electrodes on opposite sides of the quartz crystal (left), resulting in thickness shear vibration when a voltage is applied (right). *Adapted from [98]*.

The frequency of the transducer oscillation in a QCM sensor changes with mass deposited on its surface in the gas phase or vacuum according to the Sauerbrey equation [87]:

$$\Delta f = \frac{-2 f_0^2 \Delta m}{A\sqrt{\mu_q \rho_q}} = -C\Delta m$$

Where Δf is the frequency shift (Hz), f_0 is is the operating frequency of the QCM (Hz), Δm is the mass change (g), A is the active area of the QCM electrode (cm^2), μ_q is the is the shear modulus of quartz (2.947×10^{11} g cm^{-1} s^{-2}), ρ_q is the density of quartz (2.648 g cm^{-3}) and C is the integrated QCM sensitivity.

The work of Sauerbrey is considered as providing the basis for the development of QCM as an analytical tool for measuring mass. Early QCMs were applied in vacuum and gas environments, however, advancements in recent years has allowed it to be operated in liquid media where the quartz oscillator is also affected by changes in density, conductivity, temperature and viscoelasticity at the solid-liquid interface. Basically, a viscoelastic film will not fully couple to the oscillation of the crystal but instead will dampen it, a behavior that initiated the development of QCM with dissipation measurement, QCM-D, for monitoring the damping, or energy dissipation, parameter which gives information on the deposited mass layer oscillating with the sensor [99-100].

QCM has become an attractive technique and it has been used for electrochemical sensors [101], immunosensors [102], and biosensors [103]. These applications take advantage of the QCM's capacity for accurate, label-free detection of target analytes on a nanogram scale [104].

A chemical sensor or a biosensor is a device that detects and transforms chemical information into an analytically useful signal. Biosensors rely on the specific molecular interactions between the recognition element (*e.g.* antibody, enzyme or DNA) and analytes in the sample (Figure 1.9). The recognition element is connected to a transducer which then translates this bio-recognition event into a measurable signal (Figure 1.8).

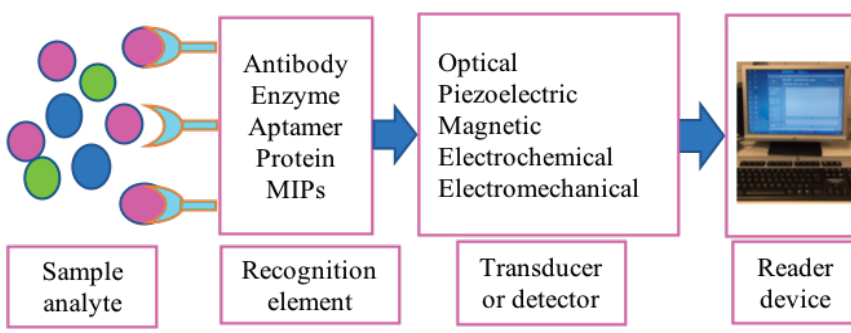

Figure 1.8. General schematic representation of a chemical sensor or a biosensor.

MIPs have recently been utilized as molecular recognition elements instead of biomolecules in chemical-sensing systems in combination with QCM transducers for the creation of powerful sensors which can be applied in clinical diagnosis, environmental analysis and enantiomeric separation [105-107]. MIP films have gained an increased interest due to their high selectivity and stability,

simple and inexpensive methods of preparation, as well as the wide range of polymer functionalities available and the easy control of film thickness.

MIPs can be immobilized on QCM transducers through two main approaches: immobilization of pre-synthesized MIP particles and *in situ* polymerization. For immobilization of MIP particles on gold surfaces, the sensor surfaces are first covered with self-assembled monolayers (SAMs) which may be composed of thiolated compounds such as 11-mercaptoundecanoic acid to introduce active groups on the gold electrode and for the improvement of the attachment of MIP particles to the modified sensor surface [108-109]. Silicon dioxide surfaces are instead covered with SAMs of organosilanes such as 3-aminopropyltriethoxysilane [110-111].

To immobilize MIPs using *in situ* polymerization, different strategies have been used including surface grafting, sandwich casting, spin coating and electro-polymerization [112-113]. In surface grafting, the sensor chip is immersed in a solution containing template, monomer and cross-linker and the application of UV irradiation results in a surface-grafted polymer film on the quartz resonator. In sandwich casting, a pre-polymerization mixture is dropped on the surface and the sensor is covered by a glass cover slide to spread the polymer solution uniformly while UV irradiation is applied. In spin coating a sensor surface containing a pre-polymerization mixture is rotated at high-speed to distribute the polymer solution evenly and thus obtain a uniform polymer layer. Electro-polymerization is performed using an electrolyte solution to prepare MIP on the surface of a sensor electrode [114].

1.4 Manipulating polymeric materials at the molecular level

Recently, there has been a tremendous increase in the use of nano and micro-scaled materials for different applications. Nature makes effective use of templates for regulating molecular-level (Ångström- and nano-scale) events in biology. The molecular self-assembly processes are essential for life in all living organisms ranging from the simplest cell to soft tissues. For instance, the cell membrane is composed mainly of phospholipid bilayers which are amphiphilic in nature, *i.e.* they contain both hydrophilic and hydrophobic regions. These bilayer membranes have many biological functions including transport, signaling and recognition between the cell and its environment. Inspired by nature, molecular self-assembly has attracted considerable attention and it has been a topic of great interest in science and technology for the

development of synthetic novel materials having hierarchical nanostructures which are able to mimic biological systems.

Amphiphiles are interesting molecules due their ability to form aggregates of different morphologies in aqueous media [115]. The self-assembly occurs depending on the amphiphile's structure and concentration, as well as the temperature and pressure. Above a certain concentration, known as the critical micelle concentration (Figure 1.9) amphiphiles tend to form micelles and further increase of concentration leads to the formation of different liquid-crystalline phases such as lamellar and normal or reverse hexagonal phases [116-119]. The driving forces acting in the amphiphiles self-assembly processes are non-covalent interactions such as hydrogen bonding, hydrophobic effects, electrostatic interactions, and van der Waals forces.

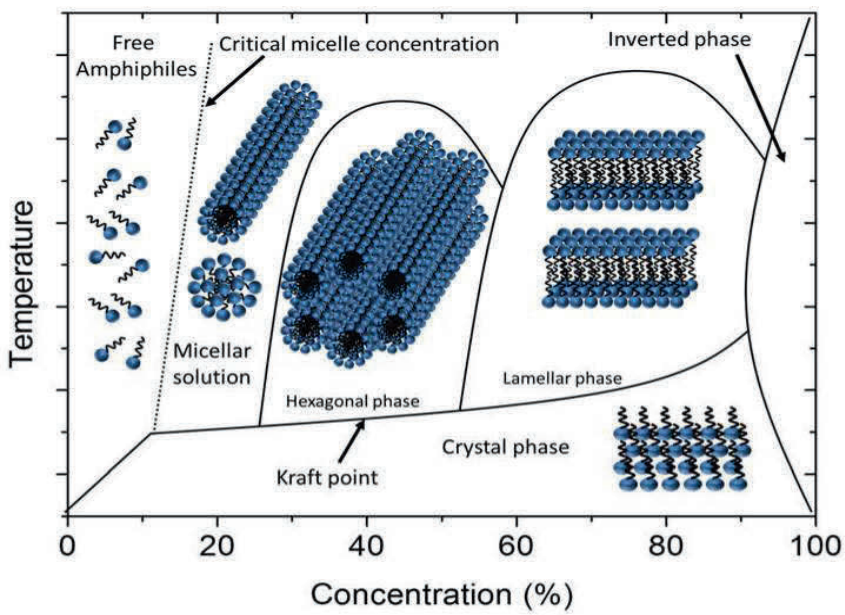

Figure 1.9. Schematic illustration of an amphiphilic surfactant dissolved in a solvent to form lyotropic liquid crystalline phases. *Reproduced from [120].*

Surfactants are examples of amphiphilic molecules widely used in many everyday products such as soaps, detergents, dispersants, cleansers, paint, paper, oil, *etc*. [121]. Depending on the nature of the hydrophilic group, conventional surfactants are classified as anionic, cationic, zwitterionic or non-ionic. An anionic surfactant has a negatively charged head group (*e.g*. sodium dodecyl sulfate (SDS) and dioctyl sodium sulfosuccinate (AOT)). A cationic

surfactant has a positively charged head group (*e.g.* cetyltrimethylammonium bromide (CTAB) and cetyltrimethylammonium chloride (CTAC)). Zwitterionic or "amphoteric" surfactants contain both cationic and anionic head groups (*e.g.* *N*-dodecyl-*N,N*-dimethyl-3-ammonio-1-propanesulfonate (SB-12)). A non-ionic surfactant bears no apparent ionic charge (*e.g.* polyoxyethylene glycol octylphenol ether (Triton X-100) and (polyethylene (7.5) tert-octylphenyl ether) (Triton X-114)) [122].

In this thesis, bottom-up strategies have been explored where liquid crystalline phases of Triton X-100/water and AOT(*p*-xylene)/water have been used for producing nanostructured MIP polymer films with high surface areas being of particular interest due to the scalability of the process and relatively inexpensive materials that are required.

Furthermore, in pursuit of more solvents capable of mediating molecular level environments in synthetic polymers, we have recently introduced the use of non-ionic deep eutectic solvents (ni-DESs) [123] for a range of applications, including their use as porogens in polymer synthesis. Over the past few decades ionic liquids (ILs) have been extensively explored owing to their unique properties such as negligible vapor pressure, high ionic conductivity, high polarity, non-volatility, recyclability, non-flammability, and high thermal, chemical, and electrochemical stability, which have made them regarded as alternatives for industrial volatile organic compounds [124]. These liquids are composed entirely of ions and are liquid at ambient or well below ambient temperature. They have been widely explored in varied applications including drug delivery [125], organic synthesis [126], polymer synthesis [127] and they have also been used in analytical processes such as separation, extraction, sensing, spectrometry and electrochemistry [128].

Deep eutectic solvents (DESs) are a class of IL analogues which are formed from a eutectic mixture of solid compounds that are not necessarily salts, such as choline chloride with hydrogen-bond donors such as urea [129-132]. A eutectic solvent is a mixture of an appropriate amount of two or more compounds that are capable of self-association to form a eutectic mixture (Figure 2.0) with a melting point/freezing point that is significantly lower than that of each individual component [133-135]. The cost, toxicity and biodegradability aspects of ionic liquids [136-140] lead to the search for alternatives and development of ni-DESs, which exhibit similar physico-chemical properties to conventional ionic liquids, however, they are ion-free, cheaper, have low toxicities and are ease to prepare [123, 141].

Soviet scientists searching for liquid fertilizers and growth promoters identified the first non-ionic deep eutectic liquid [142], a mixture of the biologically and environmentally benign substances acetamide (67%, wt) and urea (33%, wt), with melting points of 80 °C and 133 °C, respectively, and a eutectic temperature of 56 °C. Our group performed computational studies of the acetamide–urea (2:1) system and the results showed that higher-order complexes of the components were the basis for the deviation from Raoult's law that underlies the melting point depression [143]. Based upon these observations, we designed a family of amide-urea-based systems where *N*-methyl substitutions were used to attenuate interaction between the flickering cluster-like species, to produce systems with deep eutectic behavior. This series of ni-DESs (Table 1.1) include examples with sub-room temperature liquid states. In addition, these observations together with the low toxicities and the availability of these solvents from renewable sources [133] motivated studies to explore these ni-DESs in polymer synthesis and their potential use as alternatives to traditional ionic liquids and other environmentally problematic organic solvents in free-radical polymerization reactions.

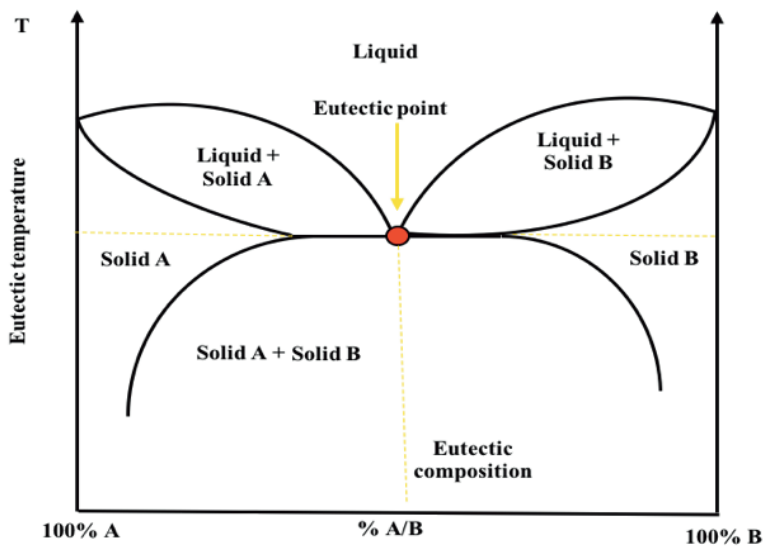

Figure 2.0. Schematic representation of temperature–composition phase diagram for a binary eutectic mixture exhibiting a eutectic point.

Table 1.1. Amide-urea eutectic combinations, their ratios and their eutectic temperatures.

Compounds with melting points (°C)	Ratios	Eutectic temperatures (°C)
Acetamide (80) – Urea (132)	65:35	56 ± 2
Acetamide (80) – *N*-methylacetamide (30)	70:30	15 ± 4
Acetamide (80) – *N*-methylurea (98-102)	50:50	42 ± 3
Acetamide (80) – *N*,*N*'-dimethylurea (101-104)	50:50	43 ± 3
N-methylacetamide (30) – *N*-methylurea (98-102)	80:20	14 ± 2
N-methylacetamide (30) – *N*,*N*'-dimethylurea (101-104)	70:30	12 ± 4

1.5 Objectives of this thesis

The primary aim of this thesis was to explore new approaches for controlling nanostructured polymer architectures and to employ these in conjunction with molecular imprinting to enhance material performance in sensor-based applications.

Two strategies were to be explored:

Firstly, to establish the feasibility of performing molecularly imprinted polymerization in liquid crystalline (LC) media, and thereafter to determine the eventual scope of the strategy.

Secondly, to determine whether a class of novel solvents, so-called “non-ionic deep eutectic solvents (ni-DESs) could be used in polymer synthesis and ultimately in conjunction with molecular imprinting strategies.

2. LIQUID CRYSTALLINE MEDIA-INFLUENCED POLYMER ARCHITECTURES

2.1 Liquid crystalline (LC) media

The use of liquid crystalline (LC) media as sacrificial templates in polymer synthesis was explored in **Papers I** and **II**. The LC-media were used for producing hierarchical architectures in molecularly imprinted polymers. The template used, the local anesthetic bupivacaine, has been extensively used in the study of many aspects of the molecular imprinting technique [144-148]. Polymer functionalities and morphologies were studied by FT-IR and SEM, respectively. The influence of the LC-media induced morphological features on the imprinted polymers was studied using QCM under flow injection analysis (FIA) conditions. In **Paper I**, the first use of LC-media in conjunction with molecular imprinting for the synthesis of hierarchical imprinted materials is presented. In **Paper II**, the scope of this strategy was explored using alternative polymers and surfactants.

Lyotrophic LC phases of Triton X-100 (TX-100, Figure 2.1, left) and AOT (Figure 2.1, right) in *p*-xylene/water were prepared using established protocols [118, 149-150]. LC TX-100 was prepared by mixing TX-100 in water (42%, v/v), then the mixture was heated at 45 °C until a homogenous phase was obtained before cooling to room temperature (18 °C). For the AOT LC phase, a 1.5 M AOT solution in *p*-xylene was prepared. The molar ratio of water to AOT was then adjusted to 15:1. The mixture was stirred continuously for 12 h to afford a homogenous phase of the viscous liquid at 18 °C.

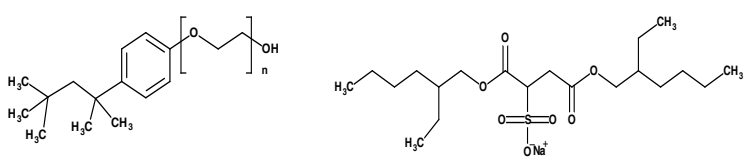

Figure 2.1. Structures of TX-100 (left) and AOT (right).

2.2 Polymer synthesis

In **Paper I**, MIP films were prepared by electropolymerization on gold-coated quartz (Au/quartz) transducers. Initially, polymerization reaction mixtures were prepared by dissolving bupivacaine hydrochloride (1 eq.) together with APBA (5 eq.) and *p*-PD (25 eq.) as cross-linking functional monomers either in ultrapure water or in TX-100 LC.

In **Paper II**, MIP films were prepared on silicon dioxide (SiO_2) coated quartz resonators by photo-chemical initiation. Bupivacaine (free base) was used as template, MAA or HEMA as functional monomer and DVB, EGDMA or BAP as cross-linker in a 1:12:55 template:monomer:cross-linker ratio. The pre-polymerization mixtures were allowed to equilibrate for complex formation in the lyotrophic LC phases of TX-100/water and AOT(*p*-xylene)/water systems. Polymer films were grown on these silanized surfaces following a strategy summarized in Figure 2.2.

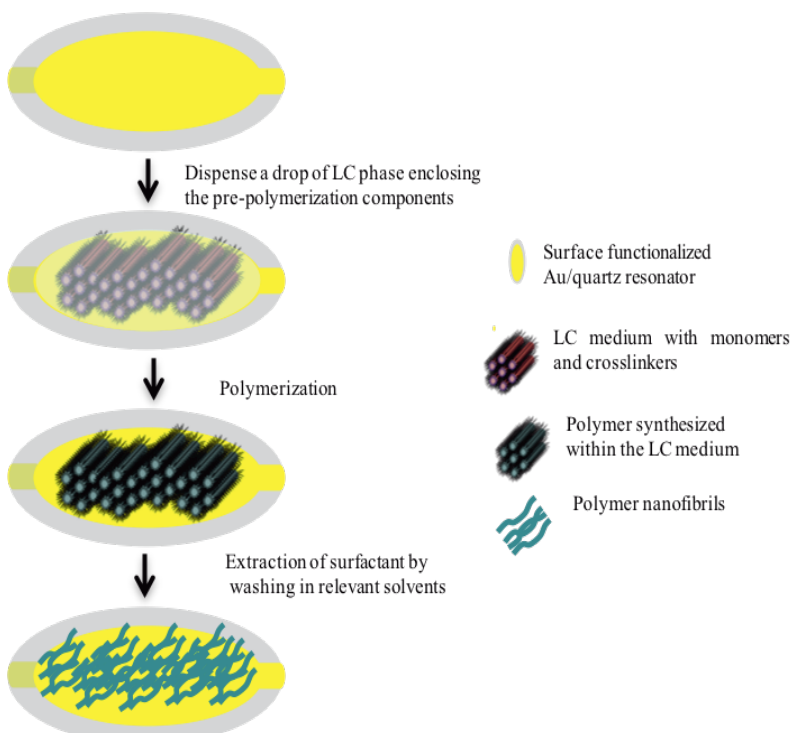

Figure 2.2. Synthesis of polymer films using liquid crystalline medium.

For the bulk polymer synthesis, thermo-initiated polymerization was performed. After polymerization, the resultant bulk polymers were crushed, ground, washed and subsequently, the particles of 63-125 μm size were collected. For comparison conventional organic or aqueous solvents were also used in polymer synthesis to serve as control for respective polymer systems.

2.3 Characterization, results and discussion of polymers synthesized in LC media

2.3.1 Identification of polymer components

The chemical functionalities of the thin polymer films and polymer monoliths were studied either by refractive angle infrared (RAIR) or by Fourier transform infrared spectroscopy (FT-IR) for the identification and verification of the presence of the anticipated polymer functionalities in both **Papers I** and **II**.

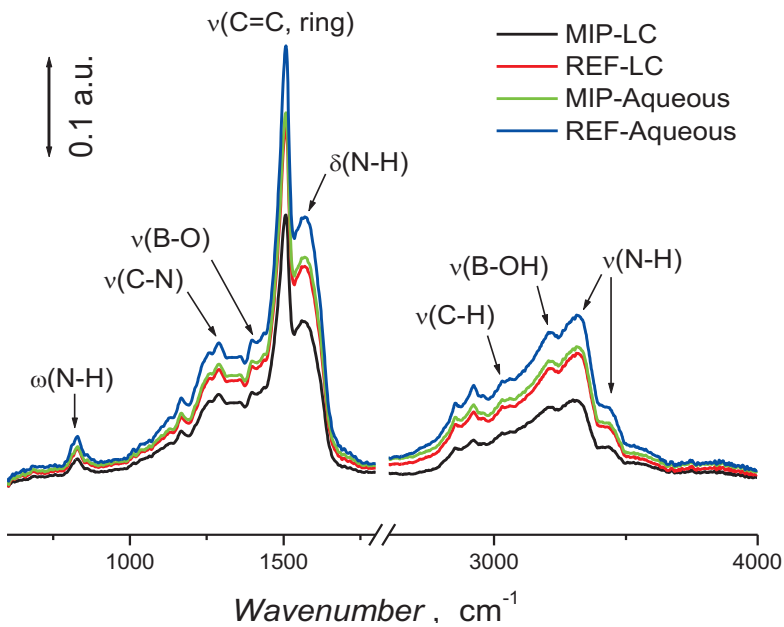

Figure 2.3. RAIR spectra of the bupivacaine MIP and REF films prepared either in the liquid crystalline media or in water.

The spectral features of MIP and REF polymer films prepared in both TX-100/water LC and water media (**Paper I**) were comparable which indicate that the template does not affect the polymerization process and the co-polymer composition. Moreover, the absence of vibrational bands for δ (C-N) around 1550 cm^{-1} and ether (C-O-C) around 1045 cm^{-1} support the conclusion that the bupivacaine template and TX-100/water LC were both efficiently removed from the polymer films (Figure 2.3).

Again, MIP and REF polymer particles (**Paper II**) prepared either in LC media or conventional solvents show comparable spectral features confirming the co-polymerization process (Figure 2.4). Importantly, no evidence of the presence of residual LC media was found. In particular, the absence of distinct spectral bands for ν (C-O-C) and ν (SO_3) around 1230 cm^{-1}, confirms the removal of TX-100/water and AOT(*p*-xylene)/water from the polymer scaffolds meaning that the LC medium acts as a sacrificial structure during the polymerization process. Interestingly, the absence of a strong band for the ν (C-N) around 1550 cm^{-1} characteristic for bupivacaine confirmed its removal.

Generally, elemental analysis results (Table 2.1) revealed comparable compositions for MIP and REF polymers prepared in the LC media. The compositions of the polymers prepared in LC media were even comparable with polymers synthesized in conventional solvents These results together with the FT-IR data indicate that the monomers are incorporated into the polymer as expected and that the presence of the LC media does not impact dramatically on polymerization. Importantly, neither of the techniques show significant differences between the compositions of the MIP and REF polymers.

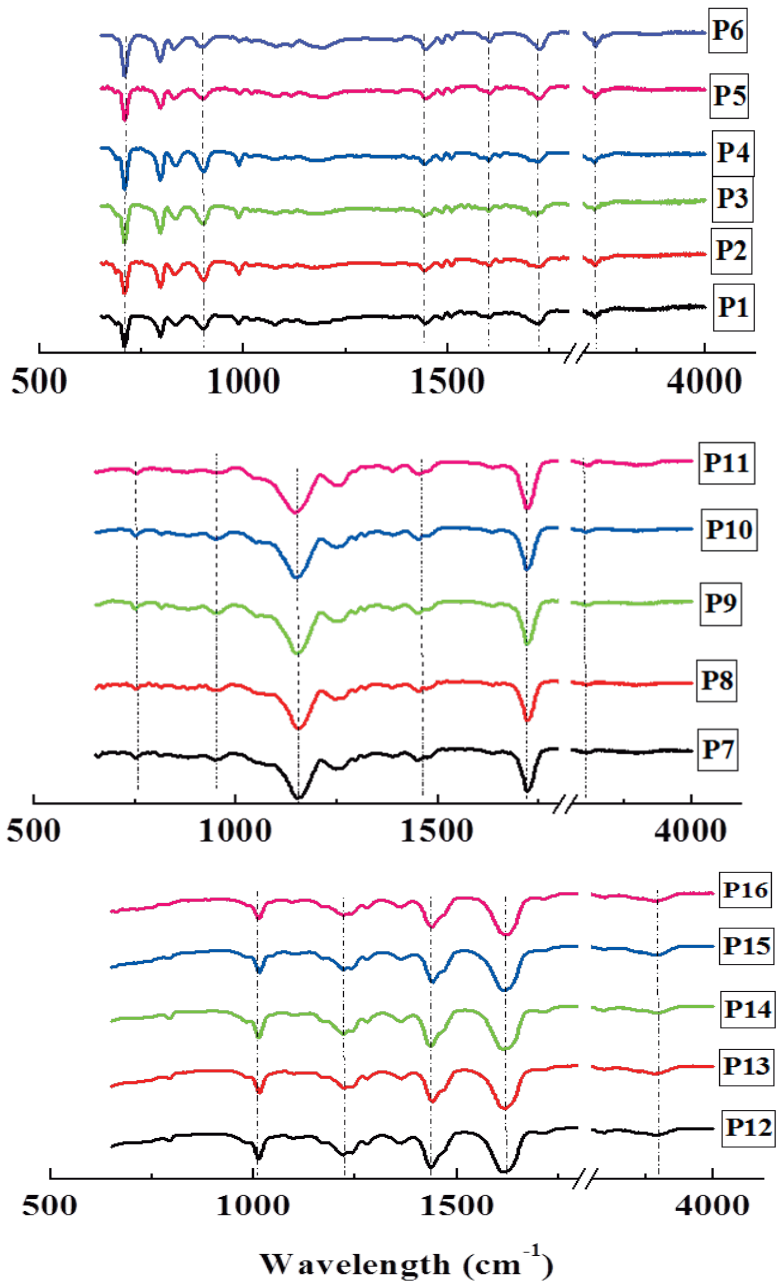

Figure 2.4. FT-IR spectra of HEMA-DVB (P1-P6), HEMA-EGDMA (P7-P11) and MAA-BAP (P12-P16) polymers prepared in different solvents.

Table 2.1. Elemental analysis of HEMA-DVB (P1-P5), HEMA-EGDMA (P6-P11) and MAA-BAP (P12-P16) polymer systems.

Polymer systems	Carbon (%)	Hydrogen (%)	Nitrogen (%)
1. MIP-HEMA-DVB-TX-100	83.7	8.5	< 0.5
2. REF-HEMA-DVB-TX-100	86.5	8.5	< 0.5
3. MIP-HEMA-DVB-AOT	84.7	8.0	< 0.5
4. REF-HEMA-DVB-AOT	86.6	8.0	< 0.5
5. REF-HEMA-DVB-TOL	84.2	8.3	< 0.5
6. MIP-HEMA-EGDMA-TX-100	58.2	7.2	< 0.5
7. REF-HEMA-EGDMA-TX-100	58.8	7.5	< 0.5
8. MIP-HEMA-EGDMA-AOT	58.9	7.0	< 0.5
9. REF-HEMA-EGDMA-AOT	58.7	7.1	< 0.5
10. REF-HEMA-EGDMA-ACETO	57.3	7.1	< 0.5
11. MIP-MAA-BAP-TX-100	53.1	7.6	10.9
12. REF-MAA-BAP-TX-100	53.7	7.9	11.1
13. MIP-MAA-BAP-AOT	54.1	7.8	11.0
14. REF-MAA-BAP-AOT	n.d.[a]		
15. REF-MAA-BAP-WATER	53.2	7.8	11.4

[a] not determined

2.3.2 Surface topography and morphology of polymers

Scanning electron microscopy (SEM) was used to examine the structure and surface morphology of 3-ABPA–*p*-PD MIP and REF polymer films are shown in Figure 2.5 (**Paper I**). Both the MIP and REF polymer films synthesized in TX-100/water LC media showed unique hexagonal cylindrical structures with organized, densely packed nanowires or brush-like structures with thickness ranging from 39.9 ± 7.8 nm and 44.6 ± 6.7 nm for MIP and REF films, respectively [151]. On the other hand, MIP and REF polymer films synthesized in aqueous media were uniform, and lacking any noticeable morphological features.

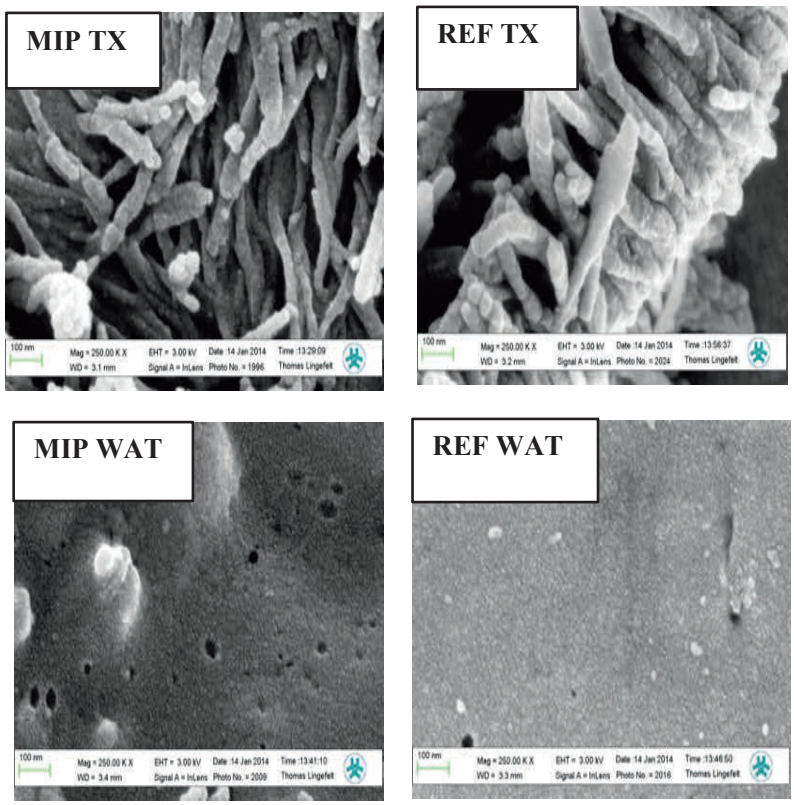

Figure 2.5. SEM topography of MIP/REF (TX) polymer films synthesized in TX-100/water LC media and MIP/REF (WAT) synthesized in water (**Paper I**).

In **Paper II**, the extended use of LC media was explored where AOT(*p*-xylene)/water reverse LC media was included together with TX-100/water in the preparation of molecularly imprinted polymers. SEM analysis results of MAA-BAP polymer systems (Figure 2.6) demonstrated hexagonal structures in both MIP and REF synthesized in AOT(*p*-xylene)/water reverse LC media compared to the films prepared in TX-100/water and water. This can be explained by the significantly higher solubility of BAP in water than in oil. As a result, the pre-polymerization mixture can be compactly packed in the hexagonal phase of the AOT(*p*-xylene)/water LC media, thus creating nanostructured patterns within the molecularly imprinted polymers patterns. In the case of TX-100/water polymer films, the pre-polymerization mixture was dispersed within the water phase of the LC medium and not inside the micelle which resulted in the lack of nanostructured morphologies.

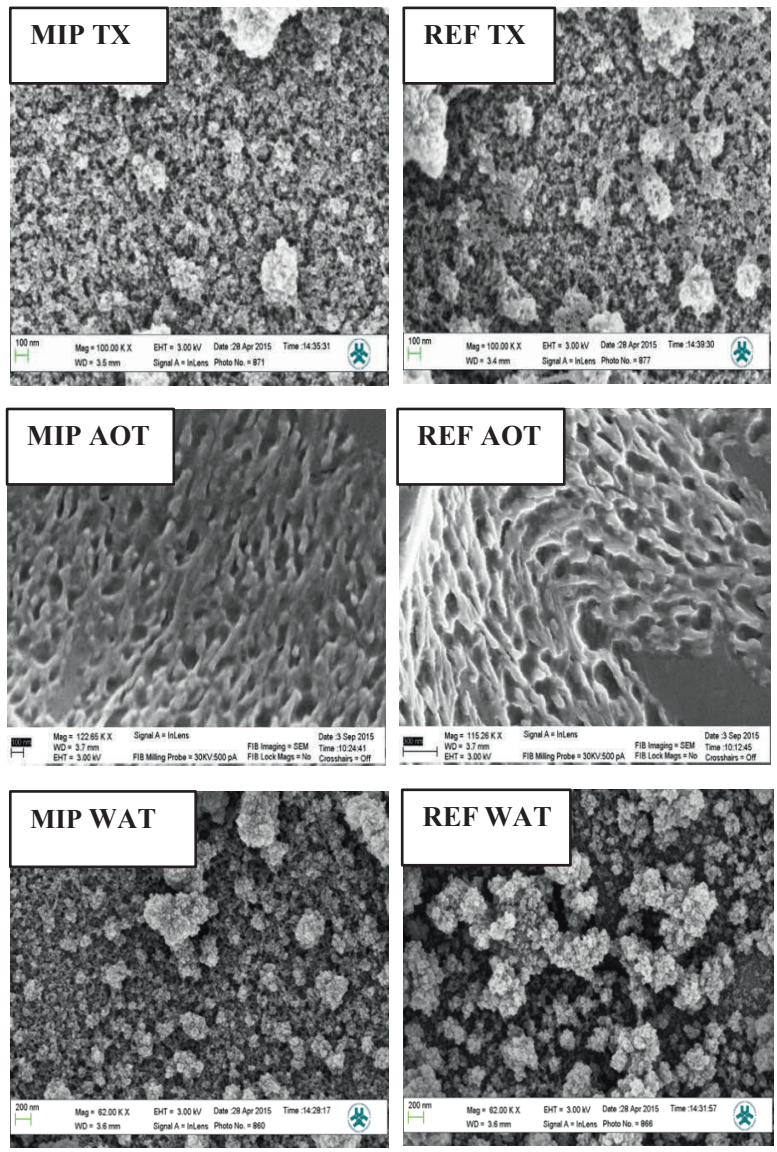

Figure 2.6. SEM micrographs of MIP/REF-MAA-BAP polymer films synthesized in TX-100/water, AOT (*p*-xylene)/water and in water (**Paper II**).

Optical microscopy analysis (OPM) was used to investigate the phase behaviour of TX-100/water, AOT(*p*-xylene)/water LC media and to study the phase behaviour of LC media before and after the addition of pre-polymerization mixtures. Figure 2.7 shows the birefringence shapes of TX-

100/water (1) and AOT(*p*-xylene)/water (4) revealing broken focal conic like textures representative of the presence of hexagonal phases. Interestingly, the optical texture was preserved when the monomers and template were added in the LC media.

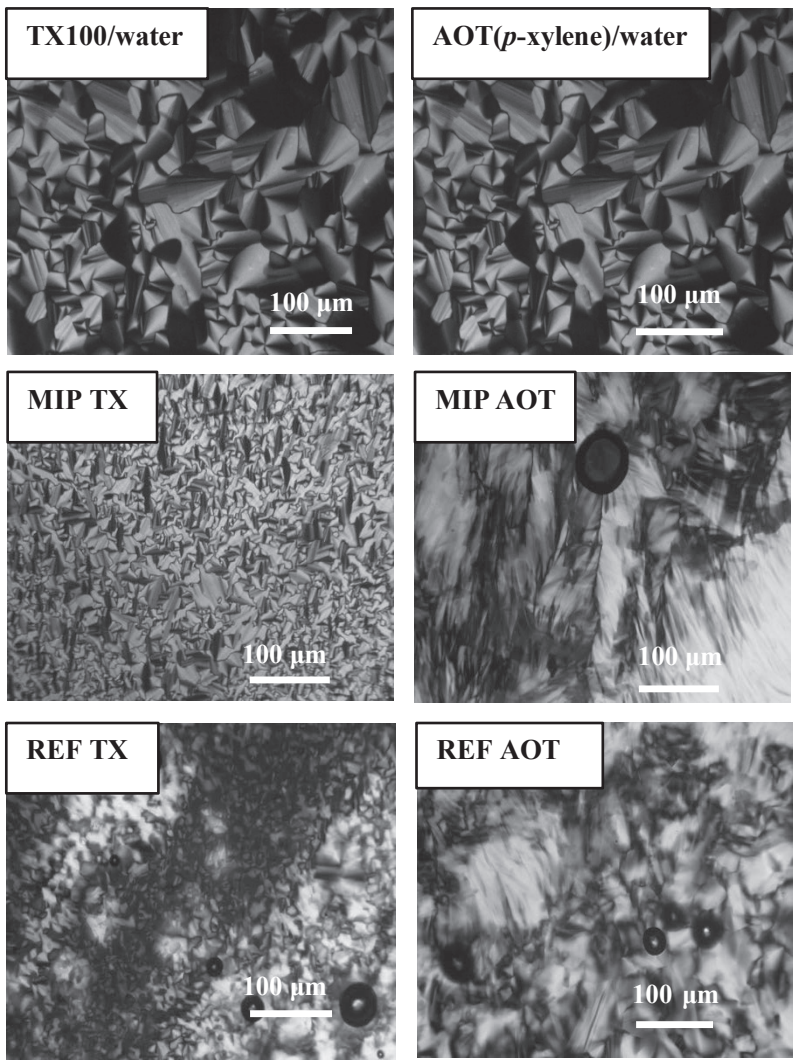

Figure 2.7. OPM images showing textures of TX100/water, MIP/REF-MAA-BAP in TX-100/water, and AOT(*p*-xylene)/water, MIP/REF-MAA-BAP in AOT(*p*-xylene)/water (**Paper II**).

2.3.3 Binding studies of synthesized polymers

The binding characteristics of the MIP and REF polymer films were assessed using a QCM system under FIA conditions. In **Paper I**, the sensitivity of polymer films synthesized either in TX-100/water LC media or in water was evaluated using a series of bupivacaine freebase concentrations. Sensitivity towards bupivacaine was four times higher for MIP LC than for REF LC as well as two and five times higher for MIP H_2O and REF H_2O, respectively (Table 2.2). The use of LC media resulted in the formation of hexagonal phases in polymer films and these polymers are anticipated to have a greater surface area, *i.e.* an increased number of accessible ligand binding cavities in close proximity to the sensor surface.

Table 2.2. Sensitivities of polymer thin films synthesized in TX-100/water and in aqueous solutions.

Polymer film	Sensitivity (Hz/mM)	Correlation coefficient for sensitivity
MIP (LC)	67.6 ± 4.9	0.995
REF (LC)	17.8 ± 2.6	0.989
MIP (H_2O)	29.9 ± 4.1	0.998
REF (H_2O)	13.2 ± 3.2	0.996

The closely related bupivacaine analogues ropivacaine and mepivacaine (Figure 1.5, having three and one carbon atoms in the *N*-alkyl side chain, respectively) were used to assess the fidelity of the binding sites in the MIP chemosensor prepared in TX-100/water LC media. The results from this QCM study are shown in Figure 2.8. They clearly show that the MIP LC film was selective with sensitivity values of two and three times higher for bupivacaine than for ropivacaine and mepivacaine, respectively (Table 2.3).

Table 2.3. Sensitivity of the MIP film prepared in TX-100 LC medium for bupivacaine and analogues.

Analyte	Sensitivity (Hz/mM)	Correlation coefficient for sensitivity
Bupivacaine	67.6 ± 4.9	0.995
Ropivacaine	38.0 ± 5.1	0.990
Mepivacaine	28.4 ± 1.5	0.989

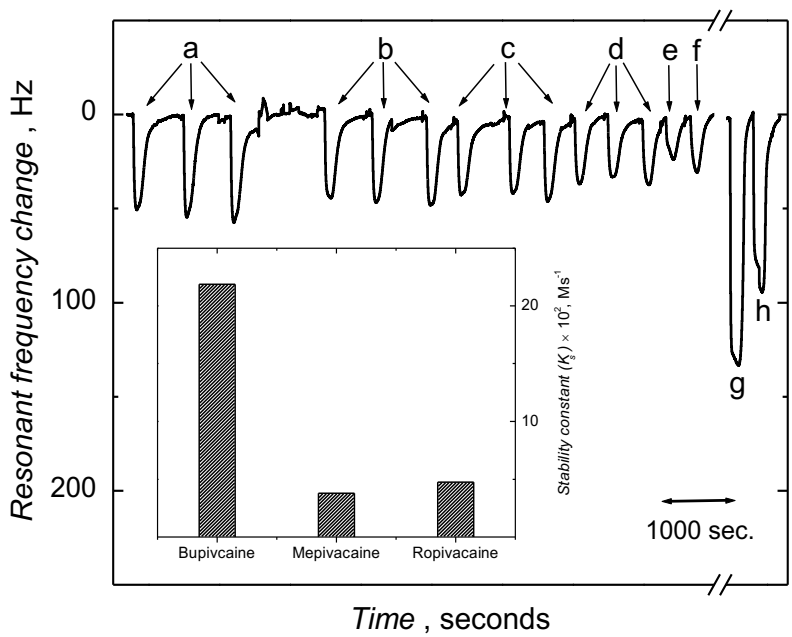

Figure 2.8. Resonant frequency *versus* time curve for bupivacaine, and analogues under FIA conditions on the MIP chemosensor prepared in TX-100/water LC media. An injection volume of 75µL was used for the analytes mepivacaine ((a) 2, (b) 1, (c) 0.7, (d) 0.5, (e) 0.3 and (f) 0.1 mM) and bupivacaine (1.7 (g) and 1 mM (h)) concentration (**Paper I**).

In **Paper II**, the imprinting capacity of the bupivacaine imprinted MAA-BAP film SiO_2 coated Au-quartz synthesized in AOT(*p*-xylene)/water LC medium was evaluated using QCM under FIA conditions. Results from this analysis (Table 2.4.) demonstrated a four-fold greater sensitivity for bupivacaine in the MIP polymer film prepared in AOT(*p*-xylene)/water LC medium, compared to the non-imprinted material prepared in the same micelle. For polymer films synthesized in TX-100/water and in water failed to show any improvement in sensitivity due to the lack of nanostructures. These results are supported by SEM images, where AOT(*p*-xylene)/water polymer systems exhibited nanostructures with thickness of 50.1 ± 9.5 nm for MIP and 37.1 ± 8.5 nm for REF AOT(*p*-xylene)/water LC in comparison to polymer films synthesized in TX-100/water or in water (Figure 2.6).

Table 2.4. Sensitivities of MAA-BAP polymer thin films synthesized in LC media and in water.

Chemosensor	Sensitivity (Hz/mM)	Correlation coefficient for sensitivity
MIP TX-100	8.2 ± 0.2	0.998
REF TX-100	4.5 ± 0.2	0.995
MIP AOT	116.0 ± 7.1	0.999
REF AOT	30.2 ± 2.5	0.997
MIP WATER	15.0 ± 0.8	0.998
REF WATER	4.5 ± 0.3	0.979

The cross-reactivity studies were carried out on the MIP-MAA-BAP polymer film synthesized in AOT(*p*-xylene)/water under FIA conditions and the resonant frequency *versus* time curve for the repetitive injections of bupivacaine and analogues is shown in figure 2.9. Results from these studies showed a noticeably higher sensitivity for bupivacaine than for its closely related analogues (Table 2.5).

Table 2.5. Sensitivities of bupivacaine imprinted MAA-BAP polymer thin films synthesized in AOT(*p*-xylene)/water reverse micelle towards structural analogues of bupivacaine.

Analyte	Sensitivity (Hz/mM)	Correlation coefficient for sensitivity
Bupivacaine	116.0 ± 7.1	0.999
Ropivacaine	20.58 ± 1.5	0.998
Mepivacaine	15.73 ± 1.3	0.999

The unique hexagonal cylindrical structures present in the LC media introduced hierarchical architectures into resultant molecularly imprinted polymers and these LC media have even been claimed to enhance the polymerization process due to improved solubility of monomers and radicals [152-153].

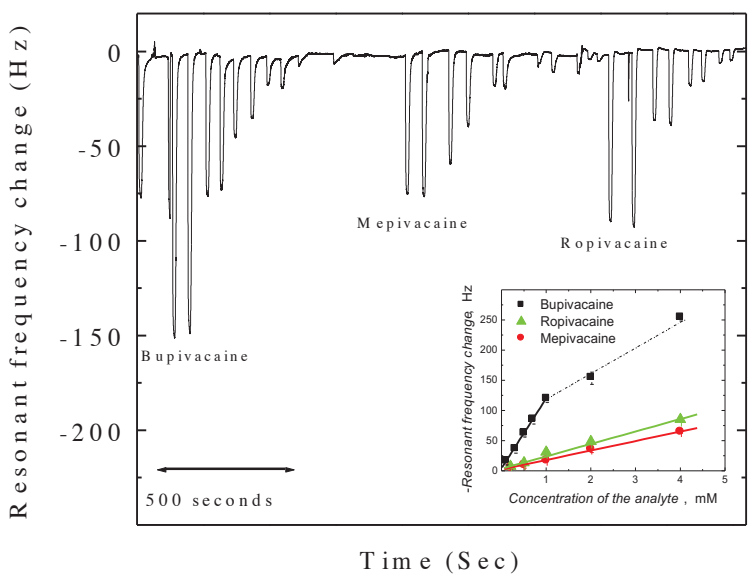

Figure 2.9. Resonant frequency *versus* time curve for the repetitive injections of bupivacaine, ropivacaine and mepivacaine under FIA conditions on MAA-BAP polymer film (**Paper II**).

2.3.4 Conclusions

Papers I and II together demonstrated the feasibility of using LC media for producing nanostructured bupivacaine-selective molecularly imprinted polymer films. The use of LC media produced polymers with high surface areas and hexagonal phases as anticipated and this improved their binding characteristics with significant enhanced sensitivities compared to the control polymers. This process is scalable and the required materials are relatively inexpensive.

Importantly, the bupivacaine imprinted polymer films prepared either in normal or reverse micelle systems exhibited high selectivities for bupivacaine over its structurally related chemical compounds analogues.

3. NON-IONIC DEEP EUTECTIC SOLVENT-INFLUENCED POLYMER ARCHITECTURES

3.1 Non-ionic deep eutectic solvents (ni-DESs)

The possibility of using the recently described ni-DESs as alternatives to conventional solvents was examined. Acetamide-urea derivative based ni-DESs (Figure 3.1) were introduced as porogens in polymer synthesis (**Paper III**) and by examining their use in molecular imprinting (**Paper IV**). These molten mixtures are cheap and eco-friendly and were used to mediate the mesoporous structure of synthetic polymers. For the first time, we have explored the application of this unique class of deep eutectic solvents (DESs) in polymer synthesis. In particular, we have deployed these solvents for the synthesis of a series of polymer films and polymer monoliths.

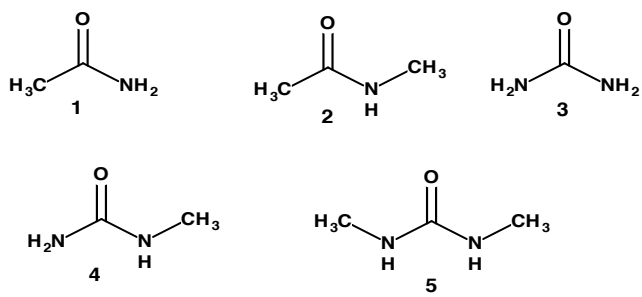

Figure 3.1. Structures of acetamide (AA, **1**), *N*-methylacetamide (NMA, **2**), urea (**3**), *N*-methylurea (NMU, **4**) and *N,N'*-dimethylurea (NN'DMU, **5**).

3.2 Polymer synthesis

In **Paper III**, three different polymers were synthesized in each of the three ni-DESs (Table 3.1). HEMA-DVB, HEMA-EGDMA and MAA-BAP polymer systems were prepared with a functional monomer:cross-linker molar ratio of 12:55 and in each case, the volume of ni-DES was 1.7 times the total volume of functional monomer and cross-linker.

Table 3.1. Polymer systems synthesized and characterized in **Paper III**.

Polymer systems	NMA -AA	NMA- NMU	NMA- NN'DMU	Conventional solvents [a]
HEMA-DVB	P1	P2	P3	P4
HEMA-EGDMA	P5	P6	P7	P8
MAA-BAP	P9	P10	P11	P12

[a]: DVB in toluene, EGDMA in acetonitrile and BAP in water.

In **Paper IV**, ni-DESs further explored to assess the broader scope of these novel solvents in polymer synthesis by examining their use in molecular imprinting. A series of polymers were synthesized in NMA-AA ni-DES (Table 3.2) using bupivacaine freebase as template, MAA or HEMA as functional monomer and either DVB, EGDMA or BAP as crosslinker with a molar ratio of 1:12:55, respectively.

Table 3.2. Polymer systems synthesized in NMA-AA ni-DES and characterized in **Paper IV**.

Polymer composition	
MIP-HEMA-DVB- NMA-AA	P1
REF-HEMA-DVB- NMA-AA	P2
MIP-HEMA-EGDMA- NMA-AA	P3
REF-HEMA-EGDMA- NMA-AA	P4
MIP-MAA-BAP- NMA-AA	P5
REF-MAA-BAP- NMA-AA	P6

In both **Papers III** and **IV**, the pre-polymerization mixture was dissolved in the eutectic mixture and following polymerization, the resultant bulk polymer was ground, sieved (63-125 μm) and washed. For comparison, the polymer systems were also synthesized using conventional organic or aqueous media and were treated using the same procedure.

3.3 Characterization, results and discussion of polymers synthesized in ni-DESs

3.3.1 Identification of polymer components

Polymerization of different polymer systems in either ni-DESs or conventional solvents afforded polymer monoliths. Results from FT-IR analyses reveal discernible bands representative of ν(C=O), ν(C-OH) and ν(CO-O) vibrational modes around 1710, 1010 and 1200-1000 cm^{-1}, respectively, indicating the presence of the anticipated functionalities.

Importantly, the polymers prepared using ni-DESs revealed spectral features comparable to those polymers prepared in conventional organic solvents and in water as well (Figures 3.2), reflecting the removal of the eutectic mixtures from the ground polymers. This was confirmed by the absence of strong primary and secondary amide stretching modes at ≈1680 cm^{-1}. Additionally, the extraction of the bupivacaine template is indicated by the absence of strong bands around 1550 cm^{-1} for the δ (C-N) mode in the cases of the imprinted polymers P1-P4 (Figure 3.3).

Elemental analysis of carbon, hydrogen and nitrogen was performed on the 12 polymer monoliths prepared in the three ni-DESs and conventional solvents. These results are indicative of comparable incorporation of monomers. In the case of the MAA-BAP polymers (P9-P12), those prepared in the various ni-DESs (P9- P11) were comparable, though P12, prepared in water, was shown to have a marginally higher carbon content, corresponding to a lower oxygen content (Table 3.3).

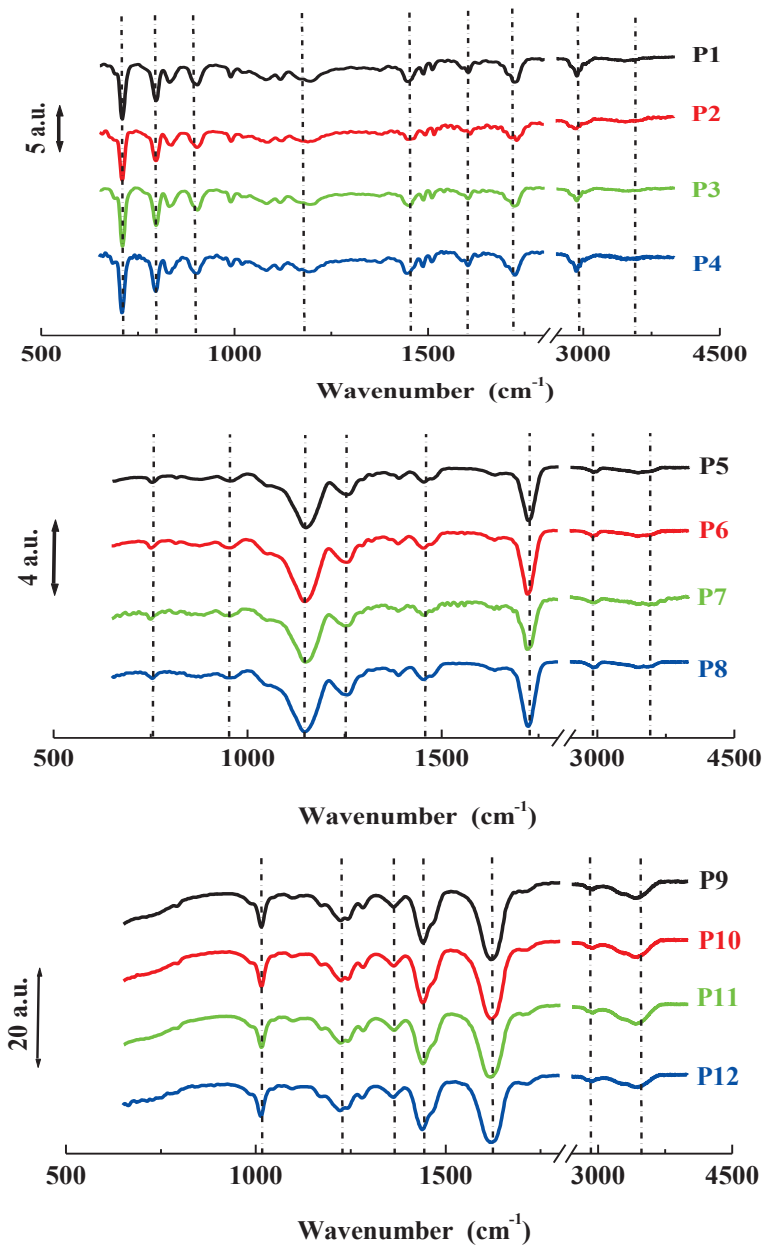

Figure 3.2. FT-IR spectra of a series of polymer particles prepared in different ni-DES: NMA-AA (black), NMA-NMU (red), NMA-NN'DMU (green) and conventional solvents (blue) (**Paper III**).

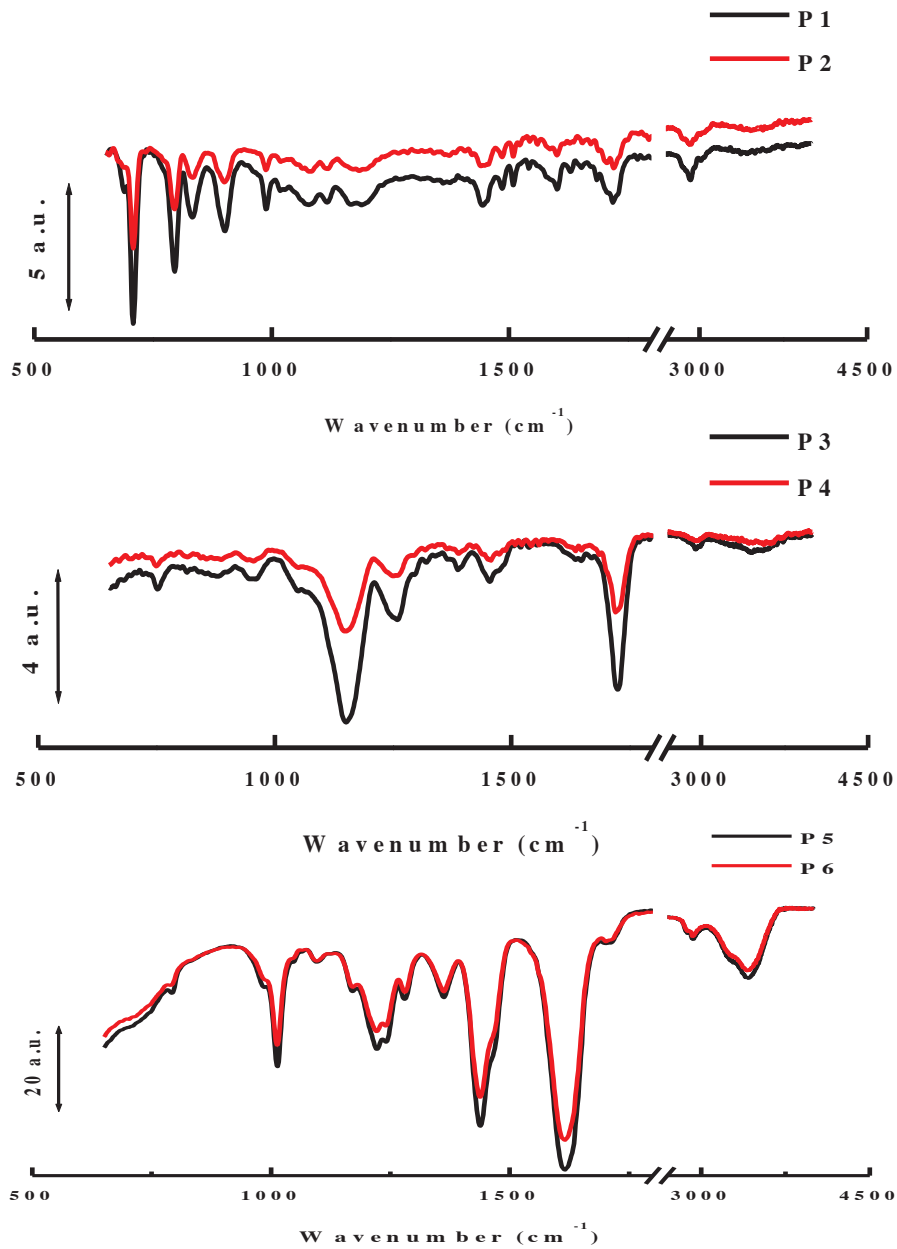

Figure 3.3. FT-IR spectra of polymers particles: HEMA-DVB (P1/P2), HEMA-EGDMA (P3/P4) and MAA-BAP (P5/P6) prepared in NMA-AA ni-DES (**Paper IV**).

Table 3.3. Elemental analysis of polymers P1-P12 (**Paper III**).

Polymers	Carbon (%)	Hydrogen (%)	Nitrogen (%)
P1	84.7	8.2	< 0.5
P2	84.7	8.2	< 0.5
P3	84.8	8.3	< 0.5
P4	84.9	8.2	< 0.5
P5	59.3	7.9	< 0.4
P6	59.9	7.4	< 0.4
P7	59.3	7.4	< 0.4
P8	59.4	7.4	< 0.4
P9	57.1	7.9	12.3
P10	57.5	8.1	12.5
P11	57.7	8.0	12.6
P12	59.4	8.0	12.6

Elemental analysis (N) of the non-nitrogen containing co-polymers (P1-P4) in NMA-AA ni-DES revealed nitrogen contents below the detection limit, < 0.4 %, indicating the effective removal of the NMA-AA during the polymer workup. Together, the elemental analysis and FT-IR data clearly show that the amide-based DESs are neither entrapped in the resultant polymers nor are they incorporated into the polymer structure. In addition, attempts to recycle these acetamide-urea ni-DESs have provided recoveries of >80%.

3.3.2 Surface topography and morphology of polymers

SEM studies were used to further assess the effect of using the ni-DESs as alternative porogens on polymer structural and morphological features (Figures: 3.4-3.6). Essentially, comparable morphologies were observed on the same polymer systems confirming that ni-DESs provide comparable structural features to those obtained when using conventional solvents and water, ranging from mesoporous monolith-like structures to mosaic microspheres.

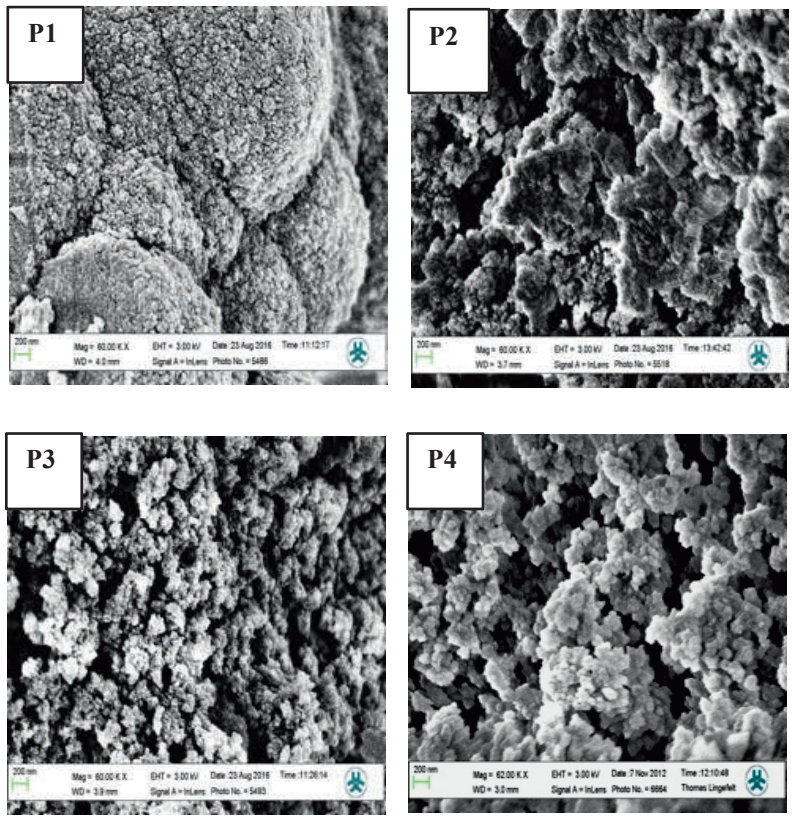

Figure 3.4. SEM images of HEMA-DVB polymer systems synthesized in NMA-AA (P1), NMA-NMU (P2), NMA-NN'DMU (P3) ni-DESs and in toluene (P4) (**Paper III**).

Polymer systems prepared with HEMA-DVB co-polymers (P1-P4) have a compact appearance with low porosity. More porous structures are shown in the case of less hydrophobic HEMA-EGDMA polymer systems (P5 to P8). This porosity becomes even more evident in MAA-BAP polymers (P9 to P12), which are significantly more porous than the other polymer systems. We interpret this trend to be a consequence of the solvation properties of the quite polar ni-DES, where the most polar monomers, MAA and BAP, are better solubilized than the less polar, in particular DVB.

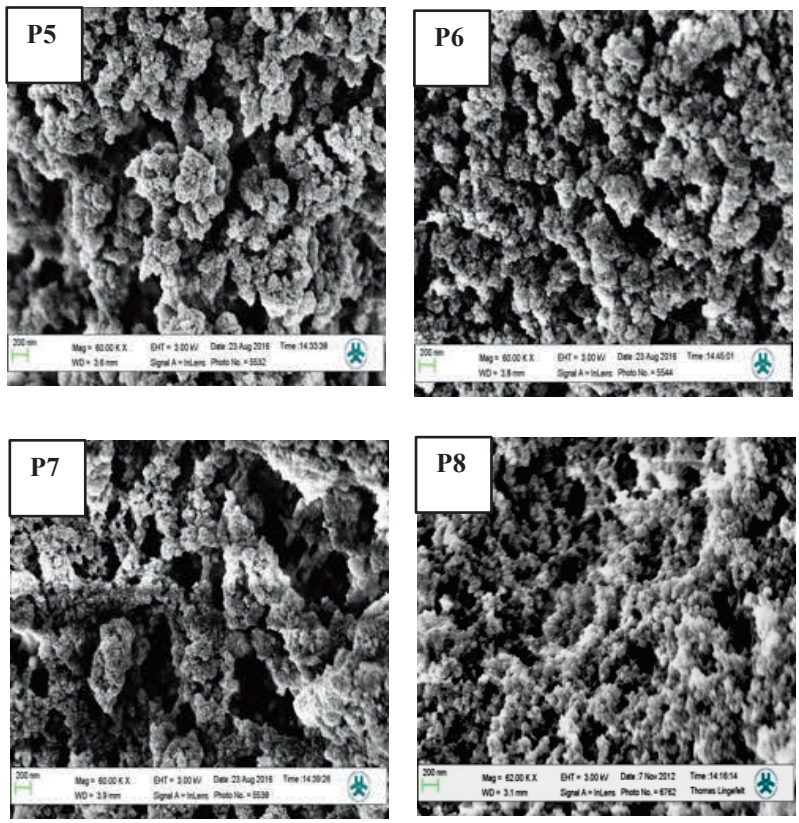

Figure 3.5. SEM images of HEMA-EGDMA polymer systems synthesized in NMA-AA (P5), NMA-NMU (P6), NMA-NN'DMU (P7) ni-DESs and in acetonitrile (P8) (**Paper III**).

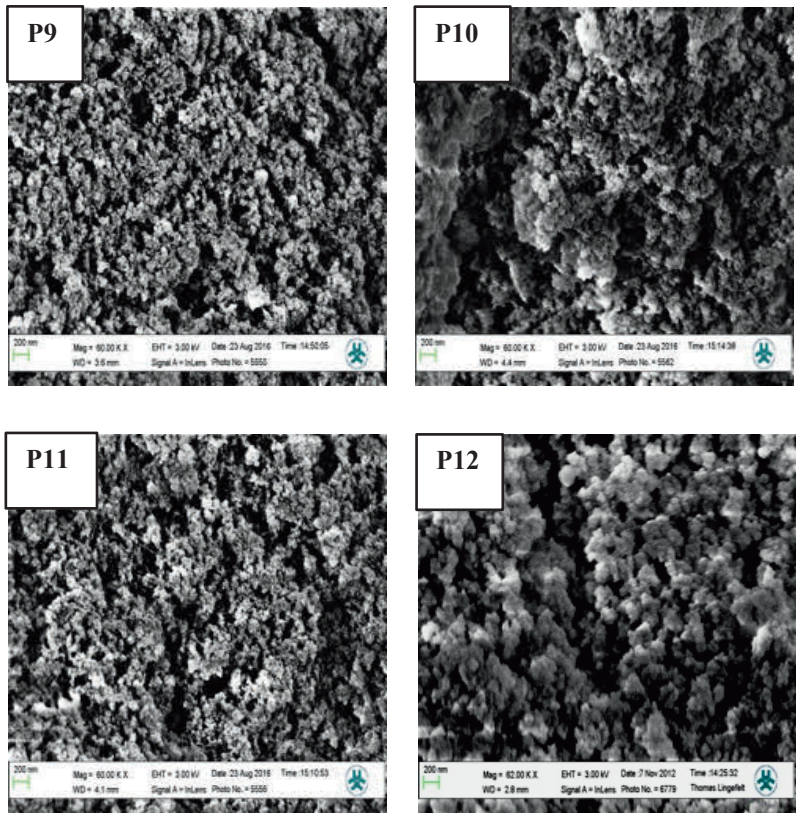

Figure 3.6. SEM images of MAA-BAP polymer particles synthesized in NMA-AA (P9), NMA-NMU (P10) and NMA-NN'DMU (P11) ni-DESs and in water (P12) (**Paper III**).

It is of particular interest that the presence of template in imprinted polymers produces no evident differences in morphology at this level, as strong comparable morphologies between imprinted and non-imprinted reference polymers are observed (Figure 3.7).

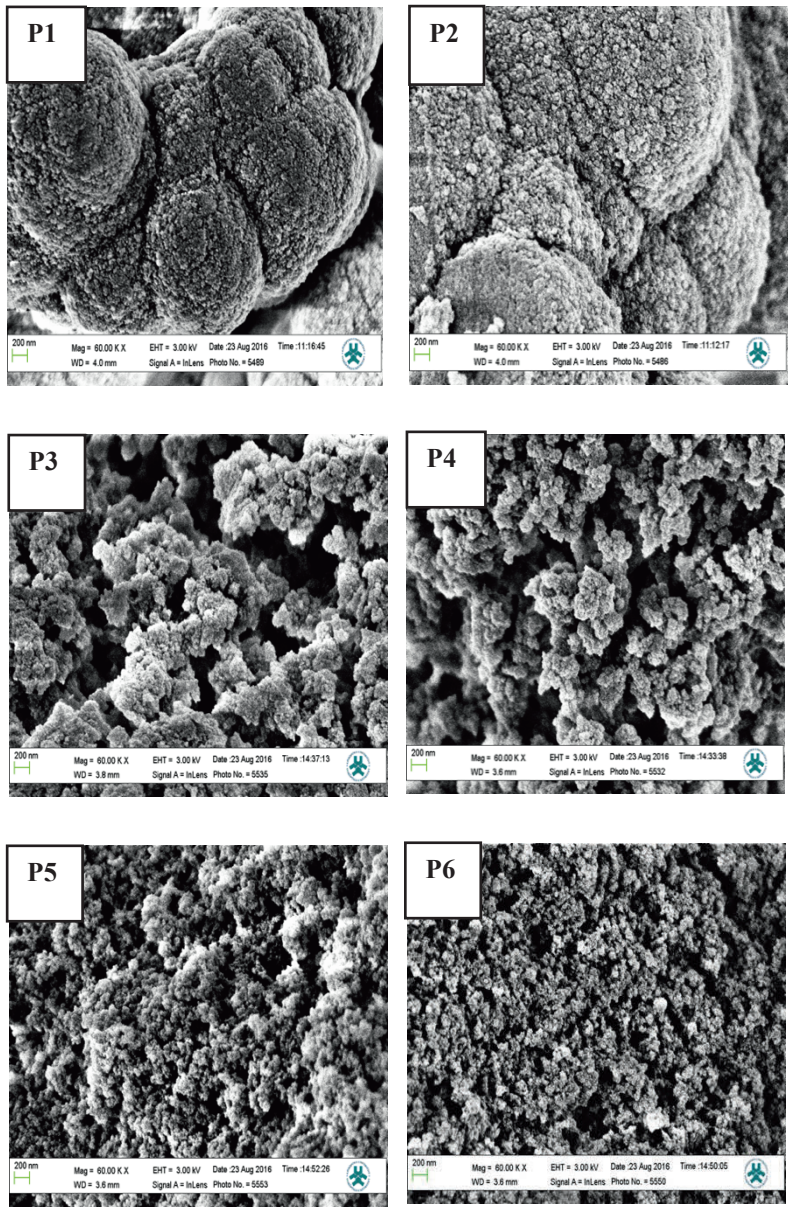

Figure 3.7. SEM images of MIP/REF-HEMA-DVB: P1/P2, MIP/REF-HEMA-EGDMA: P3/P4 and MIP/REF-MAA-BAP: P5/P6, all these polymers are synthesized in NMA-AA ni-DES (**Paper IV**).

3.3.3 Morphological studies of bulk polymers

Brunauer-Emmett-Teller (BET)-studies were used to evaluate the surface areas and porosities of the polymers. Results from these studies are shown in Figure 3.8 and table 3.5 for polymers prepared in different media (**Paper III**) and for imprinted and non-imprinted polymers prepared in NMA-AA ni-DES in Figure 3.9 and Table 3.6 (**Paper IV**). Generally, these polymer particles exhibit comparable isotherms which is type IV implying mesoporous polymer structures (2 nm < pore size > 50 nm). Some of these polymers follow a H4 hysteresis loop (associated with the secondary process of capillary condensation) indicating polymer scaffolds that are composed of mesopores that are limited by the micropores [154].

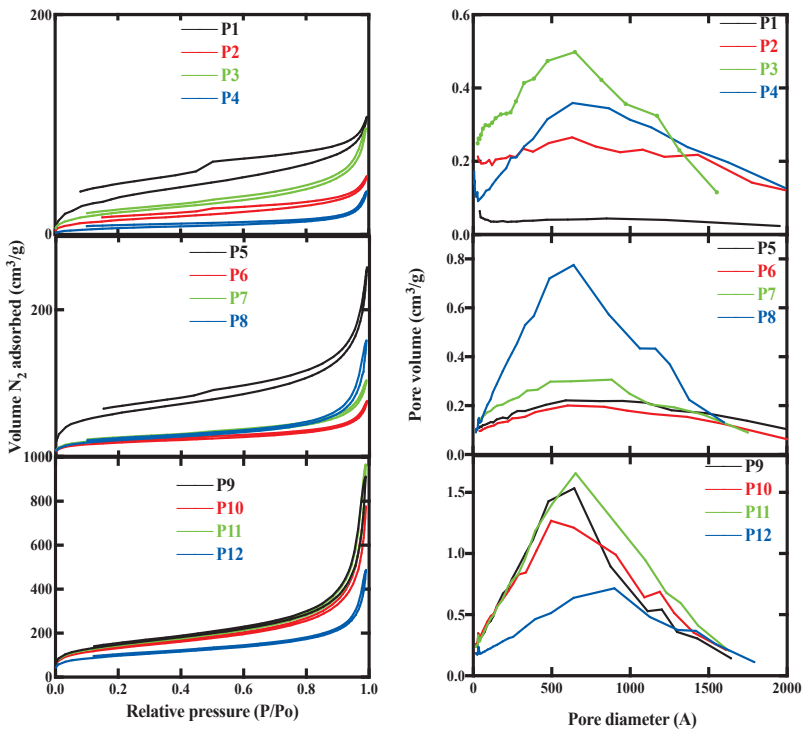

Figure 3.8. Nitrogen adsorption-desorption isotherms (left) and pore distribution plot (desorption) (right) observed from BET adsorption isotherm experiments of polymer particles prepared in ni-DESs: NMA-AA (black), NMA-NMU (red), NMA-NN'DMU (green), and in conventional solvents (blue) (**Paper III**).

Table 3.5. Surface areas and porosity parameters of the polymer particles determined with BET measurement (**Paper III**).

Polymer	Surface area (m^2/g)	Pore volume (cm^3/g)	Zeta potential (mV)
P1	127.4	0.1	-2.2
P2	234.4	0.4	0.0
P3	365.6	0.7	99.0
P4	115.0	0.3	-162.9
P5	212.4	0.3	-0.2
P6	213.7	0.3	6.6
P7	269.4	0.5	-0.8
P8	258.6	0.8	4617.6
P9	532.8	1.4	0.4
P10	477.7	1.2	-4.5
P11	516.4	1.4	-1.9
P12	335.0	0.7	68.8

In both papers, a clear trend is observed where an increase in monomer polarity resulted in a notably large surface, which we attribute to tighter hydrogen bond-driven solvation of the more polar monomers, *e.g.* MAA and BAP. On the other hand, for the DVB-based polymers, the observed relatively low surface areas reflect a poor solvation of the monomers and growing polymer chains.

Contrary to the morphological features, polymers synthesized in ni-DESs and those in conventional solvents possessed quite different zeta potentials. Polymers prepared in the ni-DESs possessed very low zeta potentials relative to those of polymers prepared in traditional solvents. This feature is indicative of relatively limited charge distribution at the surface of the ni-DES-derived polymers than for those prepared in the traditional solvents, which may be explained by a greater degree of solvatization of functionalities by the ni-DESs facilitating a more even distribution of these functionalities throughout the polymer particles.

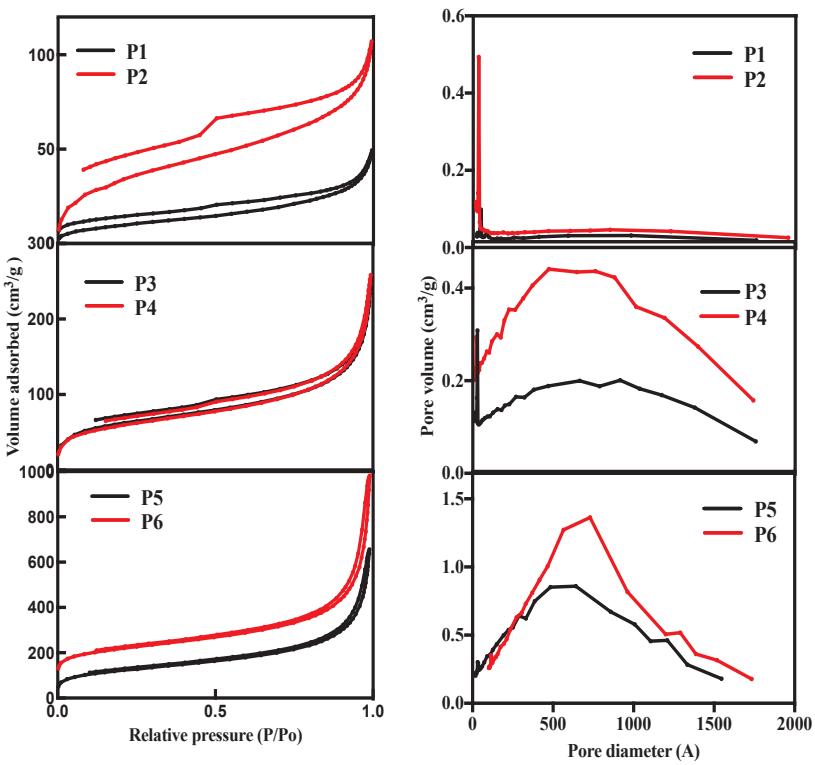

Figure 3.9. Nitrogen adsorption-desorption isotherms (left) and pore distribution plot (desorption) (right) observed from BET adsorption isotherm experiments of polymer particles MIP/REF-HEMA-DVB: P1/P2, MIP/REF-HEMA-EGDMA: P3/P4 and MIP/REF-MAA-BAP: P5/P6, all these polymers are synthesized in NMA-AA ni-DES (**Paper IV**).

Table 3.6. Surface area and porosity parameters of the bulk polymers synthesized in NMA-AA ni-DES determined with BET measurement (**Paper IV**).

Polymer	Surface area (m^2/g)	Pore volume (cm^3/g)
P1	36.7	0.0
P2	127.4	0.1
P3	221.1	0.3
P4	212.4	0.3
P5	437.6	1.1
P6	532.8	1.4

3.3.4 Binding studies of synthesized polymers

The radioligand binding studies were performed using [^{3}H]-bupivacaine in acetonitrile at room temperature to evaluate the impact of using the NMA-AA ni-DES on the molecular imprinting process by examining the template recognition properties of the resulting polymers. On account of the significant differences in surface areas of the respective imprinted and their corresponding reference polymers, binding data was normalized with respect to surface area. In general, these results from these studies showed a moderate sensitivity towards bupivacaine template (Figure 4.0).

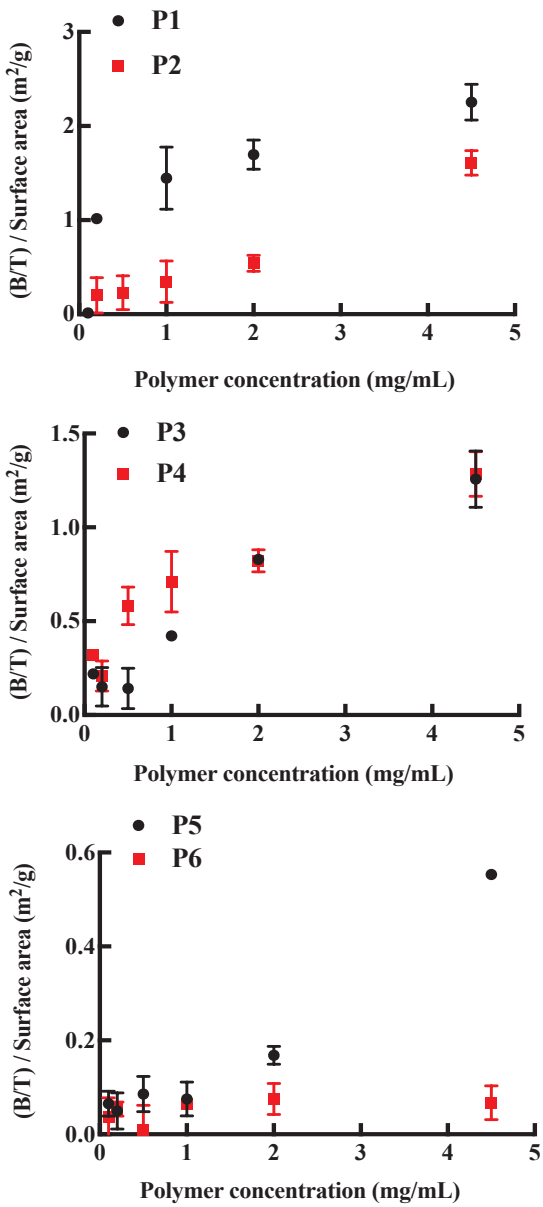

Figure 4.0. Binding of [^{3}H]-bupivacaine to HEMA-DVB (P1-P2), HEMA-EGDMA (P3-P4) and MAA-BAP (P5-P6) polymer systems synthesized in NMA-AA ni-DES (**Paper IV**).

3.3.5. Conclusions

In summary, a series of ni-DESs were shown to be useful alternatives to conventional solvents in polymer synthesis and molecular imprinting strategies. Studies of the impact of the ni–DESs on polymer morphology showed that their use with more polar components produced more porous polymers (400-500 m^2/g).

Importantly, the potential for recovery of these ni-DESs together with their low flammabilities, volatilities and toxicities can make them attractive alternatives to conventional organic solvents in many application areas, including polymer synthesis and molecular imprinting.

4. CONCLUDING REMARKS AND FUTURE OUTLOOK

In this thesis two novel strategies for influencing the properties of hierarchical polymeric materials have been explored.

Firstly, it was shown that LC media could be used in conjunction with polymer synthesis to produce polymer morphologies which had, as compared to polymers synthesized in conventional solvents. When used with molecular imprinting could generate materials with enhanced ligand recognition characteristics when used in a quartz crystal microbalance sensor format. This enhancement was attributed to the enhanced surface areas and improved The application of deep eutectic solvent ionic liquids for environmentally-friendly dissolution and recovery of precious metals mass transfer characteristics of the materials. The results from these studies highlight the potential use of these LC-based sacrificial imprinting strategies for the fabrication of polymeric materials with hierarchical architectures, which are of particular interest for use in surface-dependent application areas, *e.g.* biomaterials, catalysis or sensing.

Secondly, the first introduction of the use of ni-DESs as an alternative to conventional solvents in polymer synthesis and in molecular imprinting strategies was achieved. The use of more polar monomers (*e.g.* MAA and BAP) produced polymers with high porosity and high surface areas as compared the less polar ones. Importantly, the capacity to recover the ni-DESs after polymerization again highlights the *green* character of these economically advantageous and arguably more sustainable alternatives for ionic liquids as well as for conventional volatile or toxic organic solvents in research and in industrial scale polymer synthesis.

Finally, the new strategies for controlling the properties of hierarchical polymeric materials that have been presented in this thesis may form the basis for future developments such as in exploring biorenewable resources for developing new polymer systems for application in the development of hierarchical polymeric scaffolds.

5. ACKNOWLEDGEMENTS

First and foremost, I would like to thank my heavenly Father for the gift of life and for this great opportunity.

I am incredibly grateful to my supervisor Ian Nicholls for offering me the chance to learn a lot of things in his group. I am grateful for his encouragement, enthusiasm and expert guidance during these years. I would like to express my gratitude to my co-supervisor Subramanian Suriyanarayanan who devoted a large part of his time in guiding and supervising me in so many ways. His comments, advices and friendly attitude led the way to the successful completion of this thesis. I acknowledge my other co-supervisors Jesper Wiklander and Teodor Aastrup for their help and for revising this thesis. I thank all members of our group and the department for providing a pleasant environment to work in.

I am thankful to the love of my life, Lemy, for his love, his never-ending support and encouragement. Kenza, my sweet daughter, I just love you.

I would like to thank my lovely mum for her love, care and for encouraging me in all. Mum, you are such a great parent. I am grateful for my whole family and friends for their love, kindness and unconditional support.

Finally, I like to express my heartfelt gratitude to my belated father for his love, care, support and for encouraging me to do my best. Daddy, I dedicate this work to you and you are dearly missed.

6. REFERENCES

1. Tabor, D.P., Roch, L.M., Saikin, S.K., Kreisbeck, C., Sheberla, D., Montoya, J.H., Dwaraknath, S., Aykol, M., Ortiz, C., Tribukait, H., Amador-Bedolla, C., Brabec, C.J., Maruyama, B., Persson, K.A. & Aspuru-Guzik, A. **(2018)**. Accelerating the discovery of materials for clean energy in the era of smart automation. *Nature Reviews Materials*. 3: 5-20.

2. Kim, D.C. & Kang, D.J. **(2008)**. Molecular Recognition and Specific Interactions for Biosensing Applications. *Sensors (Basel, Switzerland)*. 8: 6605-6641.

3. Schroeder, H.W., Jr. & Cavacini, L. **(2010)**. Structure and function of immunoglobulins. *Journal of Allergy and Clinical Immunology*. 125: S41-52.

4. Lipman, N.S., Jackson, L.R., Trudel, L.J. & Weis-Garcia, F. **(2005)**. Monoclonal Versus Polyclonal Antibodies: Distinguishing Characteristics, Applications, and Information Resources. *Institute for Laboratory Animal Research Journal*. 46: 258-268.

5. Day, M.J. **(2015)**. Introduction to Antigen and Antibody Assays. *Topics in Companion Animal Medicine*. 30: 128-131.

6. Adungo, F., Yu, F., Kamau, D., Inoue, S., Hayasaka, D., Posadas-Herrera, G., Sang, R., Mwau, M. & Morita, K. **(2016)**. Development and Characterization of Monoclonal Antibodies to Yellow Fever Virus and Application in Antigen Detection and IgM Capture Enzyme-Linked Immunosorbent Assay. *Clinical and Vaccine Immunology* 23: 689-697.

7. Foltz, I.N., Karow, M. & Wasserman, S.M. **(2013)**. Evolution and emergence of therapeutic monoclonal antibodies: what cardiologists need to know. *Circulation*. 127: 2222-2230.

8. Chames, P., Van Regenmortel, M., Weiss, E. & Baty, D. **(2009)**. Therapeutic antibodies: successes, limitations and hopes for the future. *British Journal of Pharmacology*. 157: 220-233.

9. Gokel, G.W., Leevy, W.M. & Weber, M.E. **(2004)**. Crown Ethers: Sensors for Ions and Molecular Scaffolds for Materials and Biological Models. *Chemical Reviews*. 104: 2723-2750.

10. Lehn, J.-M. **(1988)**. Supramolecular Chemistry—Scope and Perspectives Molecules, Supermolecules, and Molecular Devices (Nobel Lecture). *Angewandte Chemie International Edition in English*. 27: 89-112.

11. Cram, D.J. **(1988)**. The Design of Molecular Hosts, Guests, and Their Complexes (Nobel Lecture). *Angewandte Chemie International Edition in English*. 27: 1009-1020.

12. Pedersen, C.J. **(1988)**. The Discovery of Crown Ethers (Noble Lecture). *Angewandte Chemie International Edition in English*. 27: 1021-1027.

13. http://www.nobelprize.org/nobel_prizes/chemistry/laureates/1987/. **(1987)**. The Nobel Prize in Chemistry 1987. *Nobelprize.org. Nobel Media AB 2014*.

14. Darmostuk, M., Rimpelova, S., Gbelcova, H. & Ruml, T. **(2015)**. Current approaches in SELEX: An update to aptamer selection technology. *Biotechnol Adv*. 33: 1141-1161.

15. Song, K.M., Lee, S. & Ban, C. **(2012)**. Aptamers and their biological applications. *Sensors (Basel)*. 12: 612-631.

16. Yang, X., Li, N. & Gorenstein, D.G. **(2011)**. Strategies for the discovery of therapeutic aptamers. *Expert opinion on drug discovery*. 6: 75-87.

17. Rami, A., Behdani, M., Yardehnavi, N., Habibi-Anbouhi, M. & Kazemi-Lomedasht, F. **(2017)**. An overview on application of phage display technique in immunological studies. *Asian Pacific Journal of Tropical Biomedicine*. 7: 599-602.

18. Alexander, C., Andersson, H.S., Andersson, L.I., Ansell, R.J., Kirsch, N., Nicholls, I.A., O'Mahony, J. & Whitcombe, M.J. **(2006)**. Molecular imprinting science and technology: a survey of the literature for the years up to and including 2003. *Journal of Molecular Recognition*. 19: 106-180.

19. Sellergren, B., Lepistoe, M. & Mosbach, K. **(1988)**. Highly enantioselective and substrate-selective polymers obtained by molecular imprinting utilizing noncovalent interactions. NMR and chromatographic studies on the nature of recognition. *Journal of the American Chemical Society*. 110: 5853-5860.

20. Piletsky, S.A., Piletska, E.V., Karim, K., Freebairn, K.W., Legge, C.H. & Turner, A.P.F. **(2002)**. Polymer Cookery: Influence of Polymerization Conditions on the Performance of Molecularly Imprinted Polymers. *Macromolecules*. 35: 7499-7504.

21. Piletsky, S.A., Guerreiro, A., Piletska, E.V., Chianella, I., Karim, K. & Turner, A.P.F. **(2004)**. Polymer Cookery. 2. Influence of Polymerization Pressure and Polymer Swelling on the Performance of Molecularly Imprinted Polymers. *Macromolecules*. 37: 5018-5022.

22. Batra, D. & Shea, K.J. **(2003)**. Combinatorial methods in molecular imprinting. *Current Opinion in Chemical Biology*. 7: 434-442.

23. Vasapollo, G., Sole, R.D., Mergola, L., Lazzoi, M.R., Scardino, A., Scorrano, S. & Mele, G. **(2011)**. Molecularly imprinted polymers: present and future prospective. *International Journal of Molecular Sciences*. 12: 5908-5945.

24. Yan, H. & Row, K. **(2006)**. Characteristic and Synthetic Approach of Molecularly Imprinted Polymer. *International Journal of Molecular Sciences*. 7: 155.

25. Wulff, G., Sarhan, A.-W. & Sarhan, H. **(1972)**. Use of polymers with enzyme-analogous structures for the resolution of racemates. *Angewandte Chemie International Edition* 11: 341.

26. Shea, K.J. & Thompson, E. **(1978)**. Template synthesis of macromolecules. Selective functionalization of an organic polymer. *The Journal of Organic Chemistry*. 43: 4253-4255.

27. Umpleby Ii, R.J., Bode, M. & Shimizu, K.D. **(2000)**. Measurement of the continuous distribution of binding sites in molecularly imprinted polymers. *Analyst*. 125: 1261-1265.

28. Wulff, G., Vesper, W., Grobe-Einsler, R. & Sarhan, A. **(1977)**. Enzyme-analogue built polymers, 4. On the synthesis of polymers containing chiral cavities and their use for the resolution of racemates. *Die Makromolekulare Chemie*. 178: 2799-2816.

29. Shea, K.J. & Dougherty, T.K. **(1986)**. Molecular recognition on synthetic amorphous surfaces. The influence of functional group positioning on the effectiveness of molecular recognition. *Journal of the American Chemical Society*. 108: 1091-1093.

30. Wulff, G., Best, W. & Akelah, A. **(1984)**. Enzyme-analogue built polymers, 17 Investigations on the racemic resolution of amino acids. *Reactive Polymers, Ion Exchangers, Sorbents*. 2: 167-174.

31. Arshady, R. & Mosbach, K. **(1981)**. Synthesis of substrate-selective polymers by host-guest polymerization. *Die Makromolekulare Chemie*. 182: 687-692.

32. Haupt, K., Dzgoev, A. & Mosbach, K. **(1998)**. Assay System for the Herbicide 2,4-Dichlorophenoxyacetic Acid Using a Molecularly Imprinted Polymer as an Artificial Recognition Element. *Analytical chemistry*. 70: 628-631.

33. Nicholls, I.A. **(1995)**. Thermodynamic Considerations for the Design of and Ligand Recognition by Molecularly Imprinted Polymers. *Chemistry Letters*. 24: 1035-1036.

34. Whitcombe, M.J., Rodriguez, M.E., Villar, P. & Vulfson, E.N. **(1995)**. A New Method for the Introduction of Recognition Site Functionality into Polymers Prepared by Molecular Imprinting: Synthesis and Characterization of Polymeric Receptors for Cholesterol. *Journal of the American Chemical Society*. 117: 7105-7111.

35. Wulff, G., Sarhan, A. & Zabrocki, K. **(1973)**. Enzyme-analogue built polymers and their use for the resolution of racemates. *Tetrahedron Letters*. 14: 4329-4332.

36. Caro, E., Masqué, N., Marcé, R.M., Borrull, F., Cormack, P.A.G. & Sherrington, D.C. **(2002)**. Non-covalent and semi-covalent molecularly imprinted polymers for selective on-line solid-phase extraction of 4-nitrophenol from water samples. *Journal of Chromatography A*. 963: 169-178.

37. Qi, P., Wang, J., Wang, L., Li, Y., Jin, J., Su, F., Tian, Y. & Chen, J. **(2010)**. Molecularly imprinted polymers synthesized via semi-covalent imprinting with sacrificial spacer for imprinting phenols. *Polymer*. 51: 5417-5423.

38. Biffis, A., Dvorakova, G. & Falcimaigne-Cordin, A. **(2012)**. Physical forms of MIPs. *Topics in Current Chemistry*. 325: 29-82.

39. Shoravi, S., Olsson, G.D., Karlsson, B.C., Bexborn, F., Abghoui, Y., Hussain, J., Wiklander, J.G. & Nicholls, I.A. **(2016)**. In silico screening of molecular imprinting prepolymerization systems: oseltamivir selective polymers through full-system molecular dynamics-based studies. *Org. Biomol. Chem.* 14: 4210-4219.

40. Lasáková, M. & Jandera, P. **(2009)**. Molecularly imprinted polymers and their application in solid phase extraction. *Journal of Separation Science*. 32: 799-812.

41. Piletska, E.V., Burns, R., Terry, L.A. & Piletsky, S.A. **(2012)**. Application of a molecularly imprinted polymer for the extraction of kukoamine a from potato peels. *Journal of Agricultural and Food Chemistry*. 60: 95-99.

42. Adbo, K. & Nicholls, I.A. **(2001)**. Enantioselective solid-phase extraction using Tröger's base molecularly imprinted polymers. *Analytica Chimica Acta*. 435: 115-120.

43. Sellergren, B. **(1994)**. Direct Drug Determination by Selective Sample Enrichment on an Imprinted Polymer. *Analytical chemistry*. 66: 1578-1582.

44. Kempe, M. & Mosbach, K. **(1995)**. Separation of amino acids, peptides and proteins on molecularly imprinted stationary phases. *Journal of Chromatography A*. 691: 317-323.

45. Andersson, L.I., Nicholls, I.A. & Mosbach, K., Molecular Imprinting: The Current Status and Future Development of Polymer-Based Recognition Systems, in: E.E. Bittar, B. Danielsson, L. Bülow (Eds.) Advances in Molecular and Cell Biology, Elsevier1996, pp. 651-670.

46. Sellergren, B. **(2001)**. Imprinted chiral stationary phases in high-performance liquid chromatography. *Journal of Chromatography A*. 906: 227-252.

47. Khan, H., Khan, T. & Park, J.K. **(2008)**. Separation of phenylalanine racemates using d-phenylalanine imprinted microbeads as HPLC stationary phase. *Separation and Purification Technology*. 62: 363-369.

48. Wulff, G. & Liu, J. **(2012)**. Design of Biomimetic Catalysts by Molecular Imprinting in Synthetic Polymers: The Role of Transition State Stabilization. *Accounts of Chemical Research*. 45: 239-247.

49. Wulff, G. **(2002)**. Enzyme-like Catalysis by Molecularly Imprinted Polymers. *Chemical Reviews*. 102: 1-28.

50. Anderson, C.D., Shea, K.J. & Rychnovsky, S.D. **(2005)**. Strategies for the Generation of Molecularly Imprinted Polymeric Nitroxide Catalysts. *Organic Letters*. 7: 4879-4882.

51. Liu, X.C. & Mosbach, K. **(1998)**. Catalysis of benzisoxazole isomerization by molecularly imprinted polymers. *Macromolecular Rapid Communications*. 19: 671-674.

52. Cunliffe, D., Kirby, A. & Alexander, C. **(2005)**. Molecularly imprinted drug delivery systems. *Advanced Drug Delivery Reviews*. 57: 1836-1853.

53. Norell, M.C., Andersson, H.S. & Nicholls, I.A. **(1998)**. Theophylline molecularly imprinted polymer dissociation kinetics: a novel sustained release drug dosage mechanism. *Journal of Molecular Recognition*. 11: 98-102.

54. Sellergren, B. & Allender, C.J. **(2005)**. Molecularly imprinted polymers: A bridge to advanced drug delivery. *Advanced Drug Delivery Reviews*. 57: 1733-1741.

55. Suedee, R., Srichana, T. & Martin, G.P. **(2000)**. Evaluation of matrices containing molecularly imprinted polymers in the enantioselective-controlled delivery of β-blockers. *Journal of Controlled Release*. 66: 135-147.

56. Haupt, K. & Mosbach, K. **(1998)**. Plastic antibodies: developments and applications. *Trends in Biotechnology*. 16: 468-475.

57. Vlatakis, G., Andersson, L.I., Müller, R. & Mosbach, K. **(1993)**. Drug assay using antibody mimics made by molecular imprinting. *Nature*. 361: 645.

58. Ge, Y. & Turner, A.P.F. **(2009)**. Molecularly Imprinted Sorbent Assays: Recent Developments and Applications. *Chemistry – A European Journal*. 15: 8100-8107.

59. Ye, L. & Haupt, K. **(2004)**. Molecularly imprinted polymers as antibody and receptor mimics for assays, sensors and drug discovery. *Analytical and Bioanalytical Chemistry*. 378: 1887-1897.

60. Piletsky, S.A., Piletska, E.V., Bossi, A., Karim, K., Lowe, P. & Turner, A.P.F. **(2001)**. Substitution of antibodies and receptors with molecularly imprinted polymers in enzyme-linked and fluorescent assays. *Biosensors and Bioelectronics*. 16: 701-707.

61. Vlatakis, G., Andersson, L.I., Muller, R. & Mosbach, K. **(1993)**. Drug assay using antibody mimics made by molecular imprinting. *Nature*. 361: 645-647.

62. Andersson, L.I., Müller, R., Vlatakis, G. & Mosbach, K. **(1995)**. Mimics of the binding sites of opioid receptors obtained by molecular imprinting of enkephalin and morphine. *Proceedings of the National Academy of Sciences of the United States of America*. 92: 4788-4792.

63. Andersson, L.I. **(1996)**. Application of Molecular Imprinting to the Development of Aqueous Buffer and Organic Solvent Based Radioligand Binding Assays for (S)-Propranolol. *Analytical chemistry*. 68: 111-117.

64. Haupt, K., Mayes, A.G. & Mosbach, K. **(1998)**. Herbicide Assay Using an Imprinted Polymer-Based System Analogous to Competitive Fluoroimmunoassays. *Analytical chemistry*. 70: 3936-3939.

65. Ramstrom, O., Ye, L. & Mosbach, K. **(1996)**. Artificial antibodies to corticosteroids prepared by molecular imprinting. *Chemistry and Biology*. 3: 471-477.

66. Bossi, A., Bonini, F., Turner, A.P.F. & Piletsky, S.A. **(2007)**. Molecularly imprinted polymers for the recognition of proteins: The state of the art. *Biosensors and Bioelectronics*. 22: 1131-1137.

67. Bossi, A., Piletsky, S.A., Piletska, E.V., Righetti, P.G. & Turner, A.P.F. **(2001)**. Surface-Grafted Molecularly Imprinted Polymers for Protein Recognition. *Analytical chemistry*. 73: 5281-5286.

68. Chunta, S., Suedee, R. & Lieberzeit, P.A. **(2016)**. Low-Density Lipoprotein Sensor Based on Molecularly Imprinted Polymer. *Analytical chemistry*. 88: 1419-1425.

69. Reddy, S.M., Phan, Q.T., El-Sharif, H., Govada, L., Stevenson, D. & Chayen, N.E. **(2012)**. Protein Crystallization and Biosensor Applications of Hydrogel-Based Molecularly Imprinted Polymers. *Biomacromolecules*. 13: 3959-3965.

70. Bakhshpour, M., Ozgur, E., Bereli, N. & Denizli, A. **(2017)**. Microcontact imprinted quartz crystal microbalance nanosensor for protein C recognition. *Colloids Surf B Biointerfaces*. 151: 264-270.

71. Malitesta, C., Mazzotta, E., Picca, R.A., Poma, A., Chianella, I. & Piletsky, S.A. **(2012)**. MIP sensors – the electrochemical approach. *Analytical and Bioanalytical Chemistry*. 402: 1827-1846.

72. Lee, M.-H., O'Hare, D., Chen, Y.-L., Chang, Y.-C., Yang, C.-H., Liu, B.-D. & Lin, H.-Y. **(2014)**. Molecularly imprinted electrochemical sensing of urinary melatonin in a microfluidic system. *Biomicrofluidics*. 8: 054115.

73. Haupt, K. & Mosbach, K. **(2000)**. Molecularly Imprinted Polymers and Their Use in Biomimetic Sensors. *Chemical Reviews*. 100: 2495-2504.

74. Cieplak, M. & Kutner, W. **(2016)**. Artificial Biosensors: How Can Molecular Imprinting Mimic Biorecognition? *Trends in Biotechnology*. 34: 922-941.

75. Suriyanarayanan, S., Mandal, S., Ramanujam, K. & Nicholls, I.A. **(2017)**. Electrochemically synthesized molecularly imprinted polythiophene nanostructures as recognition elements for an aspirin-chemosensor. *Sensors and Actuators B: Chemical*. 253: 428-436.

76. Algieri, C., Drioli, E., Guzzo, L. & Donato, L. **(2014)**. Bio-Mimetic Sensors Based on Molecularly Imprinted Membranes. *Sensors (Basel, Switzerland)*. 14: 13863-13912.

77. Suryanarayanan, V., Wu, C.-T. & Ho, K.-C. **(2010)**. Molecularly Imprinted Electrochemical Sensors. *Electroanalysis*. 22: 1795-1811.

78. Malitesta, C., Losito, I. & Zambonin, P.G. **(1999)**. Molecularly Imprinted Electrosynthesized Polymers: New Materials for Biomimetic Sensors. *Analytical Chemistry*. 71: 1366-1370.

79. Georgescu, B.E., Branger, C., Iordache, T.-V., Iovu, H., Vitrik, O.B., Dyshlyuk, A.V., Sarbu, A. & Brisset, H. **(2018)**. Application of unusual on/off electrochemical properties of a molecularly imprinted polymer based on an EDOT–thiophene precursor for the detection of ephedrine. *Electrochemistry Communications*. 94: 45-48.

80. Ekomo, V.M., Branger, C., Bikanga, R., Florea, A.-M., Istamboulie, G., Calas-Blanchard, C., Noguer, T., Sarbu, A. & Brisset, H. **(2018)**. Detection of Bisphenol A in aqueous medium by screen printed carbon electrodes incorporating electrochemical molecularly imprinted polymers. *Biosensors and Bioelectronics*. 112: 156-161.

81. Cenci, L., Andreetto, E., Vestri, A., Bovi, M., Barozzi, M., Iacob, E., Busato, M., Castagna, A., Girelli, D. & Bossi, A.M. **(2015)**. Surface plasmon resonance based on molecularly imprinted nanoparticles for the picomolar detection of the iron regulating hormone Hepcidin-25. *Journal of Nanobiotechnology*. 13: 51.

82. Lotierzo, M., Henry, O.Y., Piletsky, S., Tothill, I., Cullen, D., Kania, M., Hock, B. & Turner, A.P. **(2004)**. Surface plasmon resonance sensor for domoic acid based on grafted imprinted polymer. *Biosensors & bioelectronics*. 20: 145-152.

83. Sener, G., Uzun, L., Say, R. & Denizli, A. **(2011)**. Use of molecular imprinted nanoparticles as biorecognition element on surface plasmon resonance sensor. *Sensors and Actuators B: Chemical*. 160: 791-799.

84. Chen, Y.-C., Brazier, J.J., Yan, M., Bargo, P.R. & Prahl, S.A. **(2004)**. Fluorescence-based optical sensor design for molecularly imprinted polymers. *Sensors and Actuators B: Chemical*. 102: 107-116.

85. Wren, S.P., Nguyen, T.H., Gascoine, P., Lacey, R., Sun, T. & Grattan, K.T.V. **(2014)**. Preparation of novel optical fibre-based Cocaine sensors using a molecular imprinted polymer approach. *Sensors and Actuators B: Chemical*. 193: 35-41.

86. Curie, J. & Curie, P. **(1882)**. Phénomènes électriques des cristaux hémièdres à faces inclinées. *Journal de Physique Théorique et Appliquée*. 1: 245-251.

87. Marx, K.A. **(2003)**. Quartz crystal microbalance: a useful tool for studying thin polymer films and complex biomolecular systems at the solution-surface interface. *Biomacromolecules*. 4: 1099-1120.

88. Janshoff, A., Galla, H.-J. & Steinem, C. **(2000)**. Piezoelectric Mass-Sensing Devices as Biosensors—An Alternative to Optical Biosensors? *Angewandte Chemie International Edition*. 39: 4004-4032.

89. Vashist, S.K. & Vashist, P. **(2011)**. Recent Advances in Quartz Crystal Microbalance-Based Sensors. *Journal of Sensors*. 2011: 13.

90. O'Sullivan, C.K. & Guilbault, G.G. **(1999)**. Commercial quartz crystal microbalances – theory and applications. *Biosensors and Bioelectronics*. 14: 663-670.

91. Suriyanarayanan, S., Cywinski, P.J., Moro, A.J., Mohr, G.J. & Kutner, W. **(2012)**. Chemosensors based on molecularly imprinted polymers. *Topics in Current Chemistry*. 325: 165-265.

92. Alassi, A., Benammar, M. & Brett, D. **(2017)**. Quartz Crystal Microbalance Electronic Interfacing Systems: A Review. *Sensors*. 17: 2799.

93. García-Martinez, G., Bustabad, E.A., Perrot, H., Gabrielli, C., Bucur, B., Lazerges, M., Rose, D., Rodriguez-Pardo, L., Fariña, J., Compère, C. & Vives, A.A. **(2011)**. Development of a Mass Sensitive Quartz Crystal Microbalance (QCM)-Based DNA Biosensor Using a 50 MHz Electronic Oscillator Circuit. *Sensors*. 11: 7656.

94. Sagmeister, B.P., Graz, I.M., Schwodiauer, R., Gruber, H. & Bauer, S. **(2009)**. User-friendly, miniature biosensor flow cell for fragile high fundamental frequency quartz crystal resonators. *Biosensors and Bioelectronics*. 24: 2643-2648.

95. Wikipedia. **(2018, May)**. Quartz, Retrieved from https://en.wikipedia.org/wiki/Quartz.

96. Grimshaw, S. **(2003, April)**. Quartz Crystal Thin-Film Monitoring Forges Ahead, Retrieved from. https://www.photonics.com/a15653/Quartz_Crystal_Thin-Film_Monitoring_Forges_Ahead.

97. Smith, A.L. & Shirazi, H.M. **(2005)**. Principles of quartz crystal microbalance/heat conduction calorimetry: Measurement of the sorption enthalpy of hydrogen in palladium. *Thermochimica Acta*. 432: 202-211.

98. Skládal, P. **(2003)**. Piezoelectric quartz crystal sensors applied for bioanalytical assays and characterization of affinity interactions. *Journal of the Brazilian Chemical Society*. 14: 491-502.

99. Fogel, R., Limson, J. & Seshia, A.A. **(2016)**. Acoustic biosensors. *Essays in Biochemistry*. 60: 101-110.

100. Dixon, M.C. **(2008)**. Quartz Crystal Microbalance with Dissipation Monitoring: Enabling Real-Time Characterization of Biological Materials and Their Interactions. *Journal of Biomolecular Techniques* 19: 151-158.

101. Levi, M.D., Daikhin, L., Aurbach, D. & Presser, V. **(2016)**. Quartz Crystal Microbalance with Dissipation Monitoring (EQCM-D) for in-situ studies of electrodes for supercapacitors and batteries: A mini-review. *Electrochemistry Communications*. 67: 16-21.

102. Ertekin, O., Ozturk, S. & Ozturk, Z.Z. **(2016)**. Label Free QCM Immunobiosensor for AFB1 Detection Using Monoclonal IgA Antibody as Recognition Element. *Sensors (Basel)*. 16.

103. Emir Diltemiz, S., Kecili, R., Ersoz, A. & Say, R. **(2017)**. Molecular Imprinting Technology in Quartz Crystal Microbalance (QCM) Sensors. *Sensors (Basel)*. 17.

104. Dixon, M.C. **(2008)**. Quartz crystal microbalance: A useful tool for studying thin polymer films and complex biomolecular systems at the solution-surface interface. *Journal of Biomolecular Techniques*. 19: 151-158.

105. Afzal, A., Mujahid, A., Schirhagl, R., Bajwa, S., Latif, U. & Feroz, S. **(2017)**. Gravimetric Viral Diagnostics: QCM Based Biosensors for Early Detection of Viruses. *Chemosensors*. 5: 7.

106. Iglesias, R.A., Tsow, F., Wang, R., Forzani, E.S. & Tao, N. **(2009)**. Hybrid separation and detection device for analysis of benzene, toluene, ethylbenzene, and xylenes in complex samples. *Analytical chemistry*. 81: 8930-8935.

107. Haupt, K., Noworyta, K. & Kutner, W. **(1999)**. Imprinted polymer-based enantioselective acoustic sensor using a quartz crystal microbalance. *Analytical Communications*. 36: 391-393.

108. Kamra, T., Chaudhary, S., Xu, C., Montelius, L., Schnadt, J. & Ye, L. **(2016)**. Covalent immobilization of molecularly imprinted polymer nanoparticles on a gold surface using carbodiimide coupling for chemical sensing. *Journal of Colloid and Interface Science*. 461: 1-8.

109. Tsuru, N., Kikuchi, M., Kawaguchi, H. & Shiratori, S. **(2006)**. A quartz crystal microbalance sensor coated with MIP for "Bisphenol A" and its properties. *Thin Solid Films*. 499: 380-385.

110. Pasternack, R.M., Rivillon Amy, S. & Chabal, Y.J. **(2008)**. Attachment of 3-(Aminopropyl)triethoxysilane on Silicon Oxide Surfaces: Dependence on Solution Temperature. *Langmuir*. 24: 12963-12971.

111. Kolarov, F., Niedergall, K., Bach, M., Tovar, G.E.M. & Gauglitz, G. **(2012)**. Optical sensors with molecularly imprinted nanospheres: a promising approach for robust and label-free detection of small molecules. *Analytical and Bioanalytical Chemistry*. 402: 3245-3252.

112. Piacham, T., Josell, Å., Arwin, H., Prachayasittikul, V. & Ye, L. **(2005)**. Molecularly imprinted polymer thin films on quartz crystal microbalance using a surface bound photo-radical initiator. *Analytica Chimica Acta*. 536: 191-196.

113. Suriyanarayanan, S., Cywinski, P.J., Moro, A.J., Mohr, G.J. & Kutner, W. **(2012)**. Chemosensors based on molecularly imprinted polymers. *Top Curr Chem*. 325: 165-265.

114. Uludag, Y., Piletsky, S.A., Turner, A.P. & Cooper, M.A. **(2007)**. Piezoelectric sensors based on molecular imprinted polymers for detection of low molecular mass analytes. *The FEBS Journal*. 274: 5471-5480.

115. Holmberg, K., Jonsson, B., Kronberg, B. & Lindman, B. **(2002)**. Surfactants and Polymers in Aqueous Solution. *Wiley and Sons Ltd: Chichester*. 2nd Edition.

116. Israelachvili, J. **(1992)**. Intermolecular and Surface Forces. *Academic Press: London*. 2nd Edition.

117. Mountrichas, G., Petrov, P., Pispas, S. & Rangelov, S. **(2016)**. Nano-sized Polymer Structures via Self-assembly and Co-assembly Approaches. *Springer*. In: Fakirov S. (eds) Nano-size Polymers.

118. Ahir, S.V., Petrov, P.G. & Terentjev, E.M. **(2002)**. Rheology at the Phase Transition Boundary: 2. Hexagonal Phase of Triton X100 Surfactant Solution. *Langmuir*. 18: 9140-9148.

119. Giddi, H.S., Arunagirinathan, M.A. & Bellare, J.R. **(2007)**. Self-assembled surfactant nano-structures important in drug delivery: a review. *Indian Journal of Experimental Biology*. 45: 133-159.

120. Dierking, I. & Al-Zangana, S. **(2017)**. Lyotropic Liquid Crystal Phases from Anisotropic Nanomaterials. *Nanomaterials*. 7: 305.

121. Zeynep Atay, N., Yenigün, O. & Asutay, M. **(2002)**. Sorption of Anionic Surfactants SDS, AOT and Cationic Surfactant Hyamine 1622 on Natural Soils. *Water, Air, and Soil Pollution*. 136: 55-68.

122. Lombardo, D., Kiselev, M.A., Magazù, S. & Calandra, P. **(2015)**. Amphiphiles Self-Assembly: Basic Concepts and Future Perspectives of Supramolecular Approaches. *Advances in Condensed Matter Physics*. 2015: 22.

123. Suriyanarayanan, S. & Nicholls, I.A. **(2018)**. Mixtures for use as solvents and dispersants. 1850195-7.

124. Khandelwal, S., Tailor, Y.K. & Kumar, M. **(2016)**. Deep eutectic solvents (DESs) as eco-friendly and sustainable solvent/catalyst systems in organic transformations. *Journal of Molecular Liquids*. 215: 345-386.

125. Adawiyah, N., Moniruzzaman, M., Hawatulaila, S. & Goto, M. **(2016)**. Ionic liquids as a potential tool for drug delivery systems. *Medicinal Chemistry Communications*. 7: 1881-1897.

126. Handy, S.T. & Zhang, X. **(2001)**. Organic Synthesis in Ionic Liquids: The Stille Coupling. *Organic Letters*. 3: 233-236.

127. Minamimoto, H., Irie, H., Uematsu, T., Tsuda, T., Imanishi, A., Seki, S. & Kuwabata, S. **(2015)**. Polymerization of Room-Temperature Ionic Liquid Monomers by Electron Beam Irradiation with the Aim of Fabricating Three-Dimensional Micropolymer/Nanopolymer Structures. *Langmuir*. 31: 4281-4289.

128. Pandey, S. **(2006)**. Analytical applications of room-temperature ionic liquids: A review of recent efforts. *Analytica Chimica Acta*. 556: 38-45.

129. Paiva, A., Craveiro, R., Aroso, I., Martins, M., Reis, R.L. & Duarte, A.R.C. **(2014)**. Natural Deep Eutectic Solvents – Solvents for the 21st Century. *ACS Sustainable Chemistry & Engineering*. 2: 1063-1071.

130. Jenkin, G.R.T., Al-Bassam, A.Z.M., Harris, R.C., Abbott, A.P., Smith, D.J., Holwell, D.A., Chapman, R.J. & Stanley, C.J. **(2016)**. The application of deep eutectic solvent ionic liquids for environmentally-friendly dissolution and recovery of precious metals. *Minerals Engineering*. 87: 18-24.

131. Smith, E.L., Abbott, A.P. & Ryder, K.S. **(2014)**. Deep Eutectic Solvents (DESs) and Their Applications. *Chemical Reviews*. 114: 11060-11082.

132. Dai, Y., van Spronsen, J., Witkamp, G.-J., Verpoorte, R. & Choi, Y.H. **(2013)**. Ionic Liquids and Deep Eutectic Solvents in Natural Products Research: Mixtures of Solids as Extraction Solvents. *Journal of Natural Products*. 76: 2162-2173.

133. Zhang, Q., Vigier, K.D.O., Royer, S. & Jerome, F. **(2012)**. Deep eutectic solvents: syntheses, properties and applications. *Chemical Society reviews*. 41: 7108-7146.

134. Li, G., Wang, W., Wang, Q. & Zhu, T. **(2016)**. Deep Eutectic Solvents Modified Molecular Imprinted Polymers for Optimized Purification of Chlorogenic Acid from Honeysuckle. *Journal of Chromatographic Science*. 54: 271-279.

135. Tomé, L.I.N., Baião, V., da Silva, W. & Brett, C.M.A. **(2018)**. Deep eutectic solvents for the production and application of new materials. *Applied Materials Today*. 10: 30-50.

136. Tang, B. & Row, K.H. **(2013)**. Recent developments in deep eutectic solvents in chemical sciences. *Monatshefte für Chemie - Chemical Monthly*. 144: 1427-1454.

137. Collins, T. **(2001)**. Essays on science and society. Toward sustainable chemistry. *Science*. 291: 48-49.

138. Romero, A., Santos, A., Tojo, J. & Rodriguez, A. **(2008)**. Toxicity and biodegradability of imidazolium ionic liquids. *Journal of Hazardous Materials*. 151: 268-273.

139. Deetlefs, M. & Seddon, K.R. **(2010)**. Assessing the greenness of some typical laboratory ionic liquid preparations. *Green Chemistry*. 12: 17-30.

140. Pham, T.P., Cho, C.W. & Yun, Y.S. **(2010)**. Environmental fate and toxicity of ionic liquids: a review. *Water Research*. 44: 352-372.

141. Suriyanarayanan, S., Olsson, G.D., Kathiravan, S., Ndizeye, N. & Nicholls, I.A. **(2018)**. Non-ionic deep eutectic liquids – acetamide-urea derived room temperature solvents. *Nature Communications*. (Submitted).

142. Usanovich, M. **(1958)**. On the "deviations" from Raoult's law due to chemical interaction between the components *Doklady Akademii Nauk*. 120: 1304-1306.

143. Suriyanarayanan, S. & Nicholls, I.A., Mixtures for use as solvents and dispersants, **2018**, *1850195-7.*

144. Suriyanarayanan, S., Nawaz, H., Ndizeye, N. & Nicholls, I. **(2014)**. Hierarchical Thin Film Architectures for Enhanced Sensor Performance: Liquid Crystal-Mediated Electrochemical Synthesis of Nanostructured Imprinted Polymer Films for the Selective Recognition of Bupivacaine. *Biosensors*. 4: 90-110.

145. Schweitz, L., Andersson, L.I. & Nilsson, S. **(1997)**. Capillary electrochromatography with molecular imprint-based selectivity for enantiomer separation of local anaesthetics. *Journal of Chromatography A*. 792: 401-409.

146. Golker, K., Karlsson, B.C.G., Olsson, G.D., Rosengren, A.M. & Nicholls, I.A. **(2013)**. Influence of Composition and Morphology on Template Recognition in Molecularly Imprinted Polymers. *Macromolecules*. 46: 1408-1414.

147. Daryanavard, S.M., Jeppsson-Dadoun, A., Andersson, L.I., Hashemi, M., Colmsjo, A. & Abdel-Rehim, M. **(2013)**. Molecularly imprinted polymer in microextraction by packed sorbent for the simultaneous determination of local anesthetics: lidocaine, ropivacaine, mepivacaine and bupivacaine in plasma and urine samples. *Biomedical Chromatography*. 27: 1481-1488.

148. Dirion, B., Cobb, Z., Schillinger, E., Andersson, L.I. & Sellergren, B. **(2003)**. Water-Compatible Molecularly Imprinted Polymers Obtained via High-Throughput Synthesis and Experimental Design. *Journal of the American Chemical Society*. 125: 15101-15109.

149. Huang, L., Wang, Z., Wang, H., Cheng, X., Mitra, A. & Yan, Y. **(2002)**. Polyaniline nanowires by electropolymerization from liquid crystalline phases. *Journal of Materials Chemistry*. 12: 388-391.

150. Huang, L., Wang, H., Wang, Z., Mitra, A., Zhao, D. & Yan, Y. **(2002)**. Cuprite Nanowires by Electrodeposition from Lyotropic Reverse Hexagonal Liquid Crystalline Phase. *Chemistry of Materials*. 14: 876-880.

151. Cuiqing, W., Dairong, C. & Xiuling, J. **(2009)**. Lyotropic liquid crystal directed synthesis of nanostructured materials. *Science and Technology of Advanced Materials*. 10: 023001.

152. Raoof, J.-B., Ojani, R. & Hosseini, S.R. **(2011)**. Electrochemical fabrication of novel Pt/poly (m-toluidine)/Triton X-100 composite catalyst at the surface of carbon nanotube paste electrode and its application for methanol oxidation. *International Journal of Hydrogen Energy*. 36: 52-63.

153. Mackay, R.A. & Texter, J. **(1993)**. Electrochemistry in Colloids and Dispersions. *Journal of Chemical Education*. 70: A146.

154. Chang, S.-S., Clair, B., Ruelle, J., Beauchêne, J., Di Renzo, F., Quignard, F., Zhao, G.-J., Yamamoto, H. & Gril, J. **(2009)**. Mesoporosity as a new parameter for understanding tension stress generation in trees. *Journal of Experimental Botany*. 60: 3023-3030.